VIBRATION MEASUREMENTS USING CONTINUOUS SCANNING LASER DOPPLER VIBROMETRY: THEORETICAL VELOCITY SENSITIVITY ANALYSIS WITH APPLICATIONS

(CONTINUOUS SCANNING LASER DOPPLER VIBROMETRY: THEORETICAL ANALYSIS)

B. J. Halkon and S. J. Rothberg

Wolfson School of Mechanical and Manufacturing Engineering

Loughborough University, Loughborough, Leicestershire, LE11 3TU, U.K.

e-mail: b.j.halkon@lboro.ac.uk, tel: +44 (0) 1509 227589, fax: +44 (0) 1509 227648

ABSTRACT

It is readily accepted that a Laser Vibrometer measures target velocity in the direction of the incident laser beam but this measured velocity must be considered in terms of the various target velocity components. This paper begins with a review of the theoretical description of the velocity sensed by a single laser beam incident in an arbitrary direction on a rotating target undergoing arbitrary vibration. The measured velocity is presented as the sum of six terms, each the product of a combination of geometric parameters, relating to the laser beam orientation, and a combination of motion parameters – the "vibration sets".

This totally general velocity sensitivity model can be applied to any measurement configuration on any target. The model is also sufficiently versatile to incorporate time dependent beam orientation and this is described in this paper, with reference to continuous scanning Laser Doppler Vibrometry. For continuous scanning applications, the velocity sensitivity model is shown formulated in two useful ways. The first is in terms of the laser beam orientation angles, developing the original model to include time dependency in the angles, whilst the second is an entirely new development in which the model is written in terms of the mirror scan angles, since it is these which the operator would seek to control in practice.

In the original derivation, the illuminated section of the rotating target was assumed to be of rigid cross-section but, since continuous scanning measurements are employed on targets with flexible cross-sections, such as beams, panels and thin or bladed discs, the theory is developed in this paper for the first time to include provision for such flexibility.

KEYWORDS: Laser Doppler Vibrometry, scanning, tracking, velocity sensitivity, vibration measurement, rotating machinery. **PACS:** 06.30.Gv, 07.60.-j, 43.40.+s.

1. INTRODUCTION

The principle of Laser Doppler Vibrometry (LDV) relies on the detection of a Doppler shift in the frequency of coherent light scattered by a moving target, from which a time-resolved measurement of the target velocity is obtained. The Laser Vibrometer is now well established as an effective non-contact alternative to the use of a traditional contacting vibration transducer. Laser Vibrometers are technically well suited to general application but offer special benefits where certain measurement constraints are imposed, for example by the context, which may demand high frequency operation, high spatial resolution or remote transducer operation, or by the structure itself, which may be hot, light or rotating. Measurements on such structures are often cited as important applications of LDV [1].

For light structures, the extent of the local structural modification and resulting change in dynamic behaviour due to the attachment of a contacting transducer must always be considered [2]. This is significant when measurements are to be taken from several points, since the dynamic behaviour of the structure may change from one measurement to the next with the relocation of the transducer. For such situations, a non-contact vibration transducer capable of making a series of measurements across a component surface is desirable and LDV offers this possibility.

A substantial reduction in test time can be realised by automating the “relocation” of the measurement transducer and the suitability of the Laser Vibrometer to such automation was recognised at an early stage in the development of the instrument [3]. The introduction of some form of laser beam deflection (typically reflection by a mirror) and an associated control system enables the definition of the order in which the measurements are to be made and examples of the use of such scanning Laser

Vibrometers include measurements on automotive [4] and turbomachinery [5] components and assemblies.

In addition to this point-by-point operation of the scanning LDV, it is possible to configure the instrument to function in a continuous scanning mode. Continuous scans are conveniently arranged for by driving the beam deflection mirrors with continuous time variant signals, enabling the target velocity profile along a pre-determined path to be determined in a single measurement. Post-processing of the Laser Vibrometer output signal results in a series of coefficients that describe the operational deflection shape (ODS) or, where a frequency response function (FRF) is obtained, mode shape [2,6]. Straight-line, circular, small-scale circular and conical scans have all been proposed to measure various components of the vibration at various points on a target [6]. Continuous scanning is the particular focus of this paper. Throughout the remainder of this document, "scanning" LDV refers to operation in continuous scanning mode.

In rotating machinery, vibration measurement is essential and is typically performed from the earliest stages of design and development through to the condition monitoring of commissioned equipment [7]. The most common measurement is that of the vibration transmitted into a non-rotating component using a contacting transducer but, in some cases, low vibration transmission can make this unreliable [8]. Often, a non-contact transducer capable of measuring directly from any location along the rotor is desirable and LDV offers this possibility.

One of the earliest reported applications of LDV was, indeed, for axial vibration measurement directly from a rotating turbine blade [9] and more recent and typical examples include the measurement of vibration in magnetic discs [10,11] and bladed discs [12,13]. Configuration of a continuous scanning Laser Vibrometer to scan a circular profile enables the measurement of axial vibration [6,14] and of mode shapes

[15] in components such as axially flexible rotating discs. If the scan frequency is synchronised with the target rotation frequency, it is possible to perform a tracking Laser Vibrometer measurement in which the probe laser beam remains fixed on a particular point on the target [16].

This paper begins with a review of the theoretical description of the velocity sensed by a single laser beam incident in an arbitrary direction on a rotating target undergoing arbitrary motion. The totally general velocity sensitivity model illustrates that the measured velocity is dependent upon both the target velocity components and the orientation of the incident laser beam. In the original derivation, the illuminated section of the rotating target was assumed to be of rigid cross-section but, since Laser Vibrometer measurements are employed in applications where flexibility must be acknowledged, the first extension of the theory presented in this paper includes explicit provision for such flexibility.

The velocity sensitivity model is versatile enough to incorporate time dependent beam orientation and this is described with reference to a continuous scanning Laser Vibrometer measurement. The original derivation is developed to include time dependency in the beam orientation angles before being re-formulated to make use of the mirror scan angles, as it is these that the user would seek to control in practice. The advanced applications of circular scans on rotating targets and small-scale circular and conical scans on non-rotating targets are investigated as a means of illustrating the effectiveness of the model for the analysis of actual scan configurations. In particular, the origins of the additional components that occur in measured data due to instrument configuration are easily revealed using the revised velocity sensitivity model and an analysis of their influence is discussed for the first time in this paper.

2. VELOCITY SENSITIVITY ANALYSIS USING LASER BEAM ORIENTATION ANGLES

In the usual configuration, where the target beam is collected in direct backscatter, a Laser Vibrometer measures target velocity in the direction of the incident laser beam. For rotating targets, pure axial vibration measurements are obtained by careful alignment of the laser beam with the rotation axis. Provided consideration is given for the laser speckle effect [17], the measurement can be obtained in the same way as for a similar measurement on a non-rotating target. For radial vibration measurements, however, the presence of a velocity component due to the rotation itself generates significant cross-sensitivities to rotation speed fluctuation (including torsional oscillation) and motion components perpendicular to the intended measurement. Early studies acknowledged such cross-sensitivities [18,19] but these were only special cases of the recently derived totally general case [20] which is summarised in what follows.

2.1. TOTAL VELOCITY MEASURED AT A POINT BY A LASER VIBROMETER

With reference to Figure 1, the case considered is that of an axial element of a shaft of arbitrary cross-section, rotating about its spin axis whilst undergoing arbitrary, six degree-of-freedom vibration but this theory is equally applicable to any non-rotating, vibrating structure. A translating reference frame, *xyz*, maintains its direction at all times and has its origin, O, fixed to a point on the shaft spin axis with the undeflected shaft rotation axis defining the direction and position of the *z* axis. The time dependent unit vector $\hat{z}_R$ defines the changing direction of the spin axis, which deviates from the *z* axis as the shaft tilts. P is the instantaneous point of incidence of the laser beam on the shaft and is identified by the time dependent position vector $\vec{r}_P$.

The direction of the incident laser beam is described by the unit vector $\hat{b}$, which, if orientated according to the angles β and α as shown in Figure 2, is given by [20]:

$$\hat{b} = [\cos\beta\cos\alpha]\hat{x} + [\cos\beta\sin\alpha]\hat{y} - [\sin\beta]\hat{z}. \quad (1)$$

The convention used here, which all configurations analysed in terms of β and α in this paper follow, is that the laser beam orientation is described as a combination of two angles: with $\hat{b} = \hat{x}$ initially, first rotate by an angle β around $\hat{y}$, then by an angle α around $\hat{z}$. Clearly, the choice of orientation of the reference frame, *xyz*, relative to the structure lies with the user. Since β and α are finite rotations, their order must be maintained.

Provided that the illuminated axial element of the shaft can be assumed to be of rigid cross-section, the velocity measured by a laser beam, U_m, incident on the shaft surface, is given by [20]:

$$\begin{aligned} U_m = {} & \cos\beta\cos\alpha\left[\dot{x} + \left(\dot{\theta}_z + \Omega\right)y - \left(\dot{\theta}_y - \Omega\theta_x\right)z\right] \\ & + \cos\beta\sin\alpha\left[\dot{y} - \left(\dot{\theta}_z + \Omega\right)x + \left(\dot{\theta}_x + \Omega\theta_y\right)z\right] \\ & - \sin\beta\left[\dot{z} - \left(\dot{\theta}_x + \Omega\theta_y\right)y + \left(\dot{\theta}_y - \Omega\theta_x\right)x\right] \\ & - \left(y_0\sin\beta + z_0\cos\beta\sin\alpha\right)\left[\dot{\theta}_x + \Omega\theta_y\right] \\ & + \left(z_0\cos\beta\cos\alpha + x_0\sin\beta\right)\left[\dot{\theta}_y - \Omega\theta_x\right] \\ & + \left(x_0\cos\beta\sin\alpha - y_0\cos\beta\cos\alpha\right)\left[\dot{\theta}_z + \Omega\right], \end{aligned} \quad (2)$$

where $\dot{x}$, $\dot{y}$, $\dot{z}$ and *x*, *y*, *z* are the translational vibration velocities and displacements of the origin, O, in the *x*, *y*, *z* directions, $\dot{\theta}_x$, $\dot{\theta}_y$, $\dot{\theta}_z$ and θ_x, θ_y, (θ_z) are the angular vibration velocities and displacements of the shaft around the *x*, *y*, *z* axes (referred to as pitch, yaw and roll, respectively), Ω is the total rotation speed of the axial shaft element (combining rotation speed and any torsional oscillation), and (x_0, y_0, z_0) is the position of an arbitrary known point that lies along the line of the beam.

This paper will demonstrate how the arbitrary nature of the known point can be used to make the analysis of complex measurement configurations more straightforward. In particular, applications in which the laser beam is scanned are investigated by

considering a time dependent known point position. The analysis can also be developed to give the velocity sensitivity in applications in which the illuminated cross-section is flexible and this extension is the subject of this next section.

2.2. STRUCTURES WITH FLEXIBLE CROSS-SECTIONS

In the original derivation of equation (2), it was assumed that, although the shaft could be flexible, the illuminated cross-section would not undergo changes in shape during the course of the measurement. Whilst this assumption is reasonable in many situations, targets with flexible cross-sections are of particular interest when employing scanning LDV techniques and it is important to extend the original theory to include provision for such flexibility.

Consider a rotating shaft in which the illuminated axial element has a flexible cross-section. As illustrated in Figure 3, P is the instantaneous point of incidence of the laser beam on the arbitrarily deformed shaft element, identified by the position vector $\vec{r}_{P/O}$, and P_0 defines the corresponding point on the displaced but undeformed shaft element, identified by $\vec{r}_{P_0/O}$. Clearly:

$$\vec{r}_P = \vec{r}_O + \vec{r}_{P/O} = \vec{r}_O + \vec{r}_{P_0/O} + \vec{r}_f \,, \tag{3}$$

where $\vec{r}_P$ identifies the position of P relative to the fixed reference frame *XYZ*, $\vec{r}_O$ identifies the instantaneous position of the translating reference frame *xyz*, and $\vec{r}_f$ represents the deformation.

The velocity of P, $\vec{V}_P$, is therefore given by:

$$\vec{V}_P = \dot{\vec{r}}_P = \dot{\vec{r}}_O + \dot{\vec{r}}_{P_0/O} + \dot{\vec{r}}_f = \vec{V}_O + \left(\vec{\omega} \times \vec{r}_{P_0/O}\right) + \vec{V}_f \,, \tag{4}$$

where $\vec{\omega}$ is the angular velocity of P_0 about an instantaneous rotation axis passing through O. Equation (4) is similar to that which is obtained when considering the velocity of a point on a rotating shaft of rigid cross-section [20], the difference being the

term $\vec{V}_f$, which represents the deformation vibration velocity of P due to cross-section flexibility and the velocity measured by the Laser Vibrometer, U_m, can be written:

$$\begin{aligned} U_m &= \cos\beta\cos\alpha\left[\dot{x}_r(P_0)+\dot{x}_f(P)\right] \\ &+ \cos\beta\sin\alpha\left[\dot{y}_r(P_0)+\dot{y}_f(P)\right] \\ &- \sin\beta\left[\dot{z}_r(P_0)+\dot{z}_f(P)\right], \end{aligned} \tag{5}$$

where $\dot{x}_r(P_0)$, $\dot{y}_r(P_0)$, $\dot{z}_r(P_0)$ are the resultant vibration velocity components in the x, y, z directions due to rigid body vibration, given by:

$$\dot{x}_r(P_0) = \dot{x} - (\dot{\theta}_z + \Omega)(y_0 - y) + (\dot{\theta}_y - \Omega\theta_x)(z_0 - z) \tag{6a}$$

$$\dot{y}_r(P_0) = \dot{y} + (\dot{\theta}_z + \Omega)(x_0 - x) - (\dot{\theta}_x + \Omega\theta_y)(z_0 - z) \tag{6b}$$

and

$$\dot{z}_r(P_0) = \dot{z} + (\dot{\theta}_x + \Omega\theta_y)(y_0 - y) - (\dot{\theta}_y - \Omega\theta_x)(x_0 - x), \tag{6c}$$

and $\dot{x}_f(P)$, $\dot{y}_f(P)$, $\dot{z}_f(P)$ are the vibration velocity components in the x, y, z, directions due to cross-section flexibility, specific to point P. This shows that the rotor cross-section flexibility results in additional components due to the deformation velocities, which represent the difference between equations (2) and (5).

The development of equation (5) is significant and the convenience of its application in various measurement configurations that have proved useful in previous work, published by a number of researchers, will be demonstrated in what follows. In particular, the ease of application of equation (5), even for very complex arrangements, and the depth of information offered by the velocity sensitivity model will be demonstrated.

2.3. STRAIGHT-LINE SCANNING

A straight-line scanning Laser Vibrometer measurement is typically performed via the introduction of some form of laser beam deflection around one axis [2,6]. As illustrated

in Figure 4, a straight-line scan in the y direction is easily arranged for by the introduction of a mirror, which rotates about the z axis. In this case, application of equation (5) proceeds as follows.

The arbitrary known point is taken as the point of incidence of the laser beam on the beam deflection mirror, i.e. $y_0 = z_0 = 0$ and x_0 is the stand-off distance between the target and the Laser Vibrometer. The effect of the beam deflection is accounted for in the velocity sensitivity model by temporal variation of α, the laser beam orientation about the z axis. β, the laser beam orientation about the y axis, is zero. For a sinusoidal line scan of intended amplitude r_S and angular frequency Ω_S, α can be written as:

$$\alpha(t) = -\tan^{-1}\left(\frac{r_S}{x_0}\right)\sin(\Omega_S t + \phi_S), \tag{7}$$

where ϕ_S is the scan initial phase angle. Rearranging equation (5) and substituting $\beta = 0$ and α using equation (7) results in the following expression for the velocity measured during a straight-line scan in the y direction for a non-rotating target undergoing vibration associated with flexibility:

$$\begin{aligned} U_m = &\cos\left(\tan^{-1}\left(\frac{r_S}{x_0}\right)\sin(\Omega_S t + \phi_S)\right)\left[\dot{x}_f(P)\right] \\ &-\sin\left(\tan^{-1}\left(\frac{r_S}{x_0}\right)\sin(\Omega_S t + \phi_S)\right)\left[\dot{y}_f(P)\right]. \end{aligned} \tag{8}$$

In some situations, it may be possible to use small angle approximations to simplify equation (8) but the full expression is presented here for completeness. Clearly, when small angle approximations are appropriate, the first term in equation (8) reduces to $\dot{x}_f(P)$, which is the intended measurement. The second term introduces cross-sensitivity that may be significant if $\dot{y}_f(P)$ is large relative to $\dot{x}_f(P)$.

Typically, the instantaneous point of incidence of the laser beam on the target, P, effectively moves sinusoidally during scanning. If small angle approximations do not hold or if the target surface is not flat or not perpendicular to the *x* direction, then there will be some small distortion of this sinusoidal profile but this is typically of the order of fractions of a beam diameter and therefore insignificant.

A straight-line scan in the *z* direction is performed by mirror rotation about the *y* axis, as shown in Figure 5. In this case, $\alpha = 0$ and, for a similar sinusoidal scan, β is given by:

$$\beta(t) = -\tan^{-1}\left(\frac{r_S}{x_0}\right)\sin(\Omega_S t + \phi_S). \tag{9}$$

Substituting this into equation (5) will immediately result in an expression for the velocity measured during a straight-line scan in the *y* direction. Equations (7), (8) and (9) are intuitive but they are presented here as a convenient first application of equation (5) before more complex beam deflection configurations are considered.

2.4. CIRCULAR SCANNING

A circular scanning Laser Vibrometer measurement can be achieved by deflecting the laser beam through suitable angles around two orthogonal axes simultaneously, typically by using cosine and sine functions [6,15,16]. With reference to Figure 6, the scanning system optical axis is defined as being the line along which the laser beam is directed towards the target when there is "zero" beam deflection. In this particular configuration, the scanning system and target reference frames are collinear and the scanning system optical axis lies on the *z* axis of the target reference frame. The two orthogonal axes about which the beam is deflected during scanning are chosen such that the resulting probe laser beam manipulation occurs in the *x* and *y* directions in the target plane. The effect of such beam deflection is accounted for in the velocity sensitivity model by temporal variation of one or both of the beam orientation angles, and, in many

cases, temporal variation of the arbitrary known point that lies along the line of the laser beam.

2.4.1. The Idealised Scanning System

In the idealised scanning system, the laser beam deflection is performed by a single optical element, that can manipulate the beam orientation simultaneously about the x and y axes as shown schematically in Figure 6. In such a system, the known point (x_0, y_0, z_0) can be defined most conveniently as the incidence point of the laser beam on the scanning mirror. Clearly, the position of this point remains constant in time and scanning can be conveniently accounted for in the velocity sensitivity model by defining β as a constant and α as a function of time:

$$\beta = \frac{3\pi}{2} - \varepsilon = \frac{3\pi}{2} - \tan^{-1}\left(\frac{r_S}{z_0}\right) \tag{10a}$$

and

$$\alpha(t) = \Omega_S t + \phi_S\,, \tag{10b}$$

where, in this case, r_S is the intended scan radius and z_0 is the stand-off distance.

In this idealised configuration, substituting for β and α from equations (10a&b) into equation (5) results in:

$$\begin{aligned} U_m = &-\sin\left(\tan^{-1}\left(\frac{r_S}{z_0}\right)\right)\cos(\Omega_S t + \phi_S)\left[\dot{x}_r(P_0) + \dot{x}_f(P)\right] \\ &-\sin\left(\tan^{-1}\left(\frac{r_S}{z_0}\right)\right)\sin(\Omega_S t + \phi_S)\left[\dot{y}_r(P_0) + \dot{y}_f(P)\right] \\ &+\cos\left(\tan^{-1}\left(\frac{r_S}{z_0}\right)\right)\left[\dot{z}_r(P_0) + \dot{z}_f(P)\right], \end{aligned} \tag{11}$$

which is also intuitive. As for straight-line scanning, it may be appropriate to use small angle approximations to simplify equation (11) in some situations.

2.4.2. The Dual Mirror Scanning System

In commercially available scanning Laser Vibrometers, laser beam deflection is performed by the introduction of two orthogonally aligned mirrors, separated by some distance d_S, into the beam path. With reference to Figure 7, it can be seen that when the laser beam is traced back there is no single point from which it appears to originate. The most convenient known point to choose is the incidence point of the laser beam on the y deflection mirror, which scans back and forth along the mirror rotation axis. In addition, modulations in both β and α occur as a result of rotation of the x and y deflection mirrors, respectively. Again, the velocity sensitivity model is sufficiently versatile to be able to account for this.

The time dependency in the chosen known point x coordinate, x_0, is given by:

$$\Delta x_0(t) = \frac{r_S d_S}{z_0}\cos(\Omega_S t + \phi_S). \tag{12}$$

It can be seen from Figure 7 that equations (10a&b) must be rewritten to incorporate the modulation of β and α necessary to scan a circle, i.e.:

$$\beta(t) = \frac{3\pi}{2} - \varepsilon(t) = \frac{3\pi}{2} - \tan^{-1}\left(\frac{\sqrt{(x_S(t) - \Delta x_0(t))^2 + (y_S(t))^2}}{z_0}\right), \tag{13a}$$

and

$$\alpha(t) = \Omega_S t + \phi_S + \delta(t) = \Omega_S t + \phi_S + \tan^{-1}\left(\frac{x_S(t)}{y_S(t)}\right) - \tan^{-1}\left(\frac{x_S(t) - \Delta x_0(t)}{y_S(t)}\right), \tag{13b}$$

where the time dependency in ε and the appearance of $\delta(t)$ are readily seen as being directly related to the time dependency in x_0.

Substituting for β and α in equation (5) using equations (13a&b) will immediately result in a full expression for the velocity measured during a circular scan on a rotating, flexible target undergoing 6 degree-of-freedom vibration. It is clear, however, that this expression will not be as simple as those in the previous, simpler or idealised

applications were. Furthermore, it is the beam deflection mirror scan angles, not the laser beam orientation angles, that are controlled in real scanning systems and it is more appropriate, therefore, to re-express the velocity sensitivity model in terms of these.

3. VELOCITY SENSITIVITY ANALYSIS USING DEFLECTION MIRROR SCAN ANGLES

In the two straight-line examples described in section 2.3, the laser beam orientation angles can easily be related to the mirror scan angles. Similarly in section 2.4.1, calculating the mirror scan angles for a circular scan performed using an idealised scanning system is equally straightforward. In the case of the dual mirror system, however, the relationship between the mirror scan angles and the beam orientation angles is more complex. It is therefore more convenient to recalculate the beam orientation unit vector, $\hat{b}$, in terms of the mirror scan angles and this is described in the next section.

3.1. LASER BEAM ORIENTATION IN TERMS OF DEFLECTION MIRROR SCAN ANGLES

With reference to Figures 8 and 9, the "zero" positions of the *x* and *y* deflection mirrors which result in deflection of the laser beam along the *z* axis are both 45° (to the *y* direction). The mirror scan angles, θ_{Sx} and θ_{Sy}, are defined as positive if anticlockwise about an axis in the *z* direction and the *x* axis respectively and can be described by the unit vectors $\hat{u}_{nx}$ and $\hat{u}_{ny}$ which are normal to the mirror reflective surface.

With reference to Figure 9, it is possible to express $\hat{u}_{nx}$ and $\hat{u}_{ny}$ in terms of the principal unit vectors, $\hat{x}$, $\hat{y}$ and $\hat{z}$, as follows:

$$\hat{u}_{nx} = [\sin(45-\theta_{Sx})]\hat{x} + [\cos(45-\theta_{Sx})]\hat{y} \tag{14a}$$

and

$$\hat{u}_{ny} = -\left[\sin\left(45 - \theta_{Sy}\right)\right]\hat{y} - \left[\cos\left(45 - \theta_{Sy}\right)\right]\hat{z} . \tag{14b}$$

Let $\hat{b}_x$ be the direction of the laser beam before reflection at the *x* deflection mirror, $\hat{b}_y$ be the direction of the laser beam before reflection at the *y* deflection mirror. The convention used is that the direction of the unit vectors is from the target to the Laser Vibrometer (along the beam path), as shown in Figure 9.

Figure 9a shows the view of the reflection at the *x* deflection mirror in the negative *z* direction, illustrating that:

$$\hat{b}_y = \hat{b}_x - 2\left[\hat{b}_x \cdot \hat{u}_{nx}\right]\hat{u}_{nx} = \hat{x} - 2\left[\hat{x} \cdot \hat{u}_{nx}\right]\hat{u}_{nx} , \tag{15}$$

since in this configuration $\hat{b}_x = \hat{x}$. Similarly, Figure 9b shows the view of the reflection at the *y* deflection mirror in the negative *x* direction, illustrating that:

$$\hat{b} = \hat{b}_y - 2\left[\hat{b}_y \cdot \hat{u}_{ny}\right]\hat{u}_{ny} = \hat{x} - 2\left[\hat{x} \cdot \hat{u}_{nx}\right]\hat{u}_{nx} - 2\left[\left(\hat{x} - 2\left[\hat{x} \cdot \hat{u}_{nx}\right]\hat{u}_{nx}\right) \cdot \hat{u}_{ny}\right]\hat{u}_{ny} . \tag{16}$$

Since, as can be seen in equation (14b), $\hat{u}_{ny}$ is always perpendicular to $\hat{x}$, equation (16) can be re-written as:

$$\hat{b} = \left[\sin 2\theta_{Sx}\right]\hat{x} - \left[\cos 2\theta_{Sx} \sin 2\theta_{Sy}\right]\hat{y} + \left[\cos 2\theta_{Sx} \cos 2\theta_{Sy}\right]\hat{z} . \tag{17}$$

Equation (17) is of great significance since it defines the incident laser beam direction for any combination of deflection mirror scan angles and, as will be shown in the next section, it can be used to define the probe laser beam position in the target plane.

3.2. ARBITRARY SCAN PROFILES

With reference to Figure 8, the position of the time dependent point of incidence of the laser beam on the target, $\vec{r}_P$, can be described by x_S and y_S (omitting the explicit declaration of time dependency for brevity in the equations):

$$\vec{r}_P = \left[x_S\right]\hat{x} + \left[y_S\right]\hat{y} . \tag{18}$$

Consideration of the time dependent positions of the mirror incidence points and the target incidence point enables this to be re-expressed in terms of the time dependent mirror scan angles θ_{Sx} and θ_{Sy}. Since, as can be seen from Figure 8, the time dependency in the known point *x* coordinate is a function of the *x* deflection mirror angle, given by:

$$\Delta x_0 = -d_S \tan 2\theta_{Sx}, \tag{19}$$

the laser beam incidence point can be evaluated as follows:

$$x_S = \Delta x_0 - n\left(\hat{b} \cdot \hat{x}\right) = -d_S \tan 2\theta_{Sx} - n \sin 2\theta_{Sx}, \tag{20a}$$

$$y_S = -n\left(\hat{b}.\hat{y}\right) = n \cos 2\theta_{Sx} \sin 2\theta_{Sy} \tag{20b}$$

and

$$z_0 = n\left(\hat{b}.\hat{z}\right) = n \cos 2\theta_{Sx} \cos 2\theta_{Sy}, \tag{20c}$$

where *n* is the distance between the *y* deflection mirror and the target along the line of the laser beam. Substitution for *n* from equation (20c) into equations (20a&b) results in a totally general description of the point of incidence of the laser beam for any combination of mirror scan angles:

$$x_S = -\tan 2\theta_{Sx}\left(d_S + \frac{z_0}{\cos 2\theta_{Sy}}\right) \tag{21a}$$

and

$$y_S = z_0 \tan 2\theta_{Sy}. \tag{21b}$$

Whilst equation (21b) can be rearranged such that the *y* deflection mirror scan angle can be obtained for any y_S, it can be seen from equation (21a) that x_S is not a simple function of the *x* deflection mirror scan angle. This is particularly important when attempting to obtain a circular scan profile via the simultaneous modulation of the *x* and *y* deflection mirror scan angles.

3.3. CIRCULAR SCAN PROFILES

As illustrated in Figure 8, a circular scan profile in the target plane, with radius r_S, scan angular frequency Ω_S and initial phase ϕ_S, requires that x_S and y_S are cosine and sine functions, respectively, such that equation (18) can be re-written as:

$$\vec{r}_P = [x_S]\hat{x} + [y_S]\hat{y} = [r_S \cos(\Omega_S t + \phi_S)]\hat{x} + [r_S \sin(\Omega_S t + \phi_S)]\hat{y}\,. \tag{22}$$

Substituting for x_S and y_S in equations (21a) and (21b) results in two equations which must be rearranged for the deflection mirror scan angles if such a scan profile is to be achieved. This rearrangement is not possible for equation (21a), the consequence of which is that a perfect circular scan cannot be achieved using basic functions to drive the deflection mirrors.

3.3.1. Typical Deflection Mirror Scan Angles

If cosine and sine functions of equal amplitude are used to perform a "circular" scan, i.e.:

$$\theta_{Sx} = -\Theta_{Sx} \cos(\Omega_S t + \phi_S) \tag{23a}$$

and

$$\theta_{Sy} = \Theta_{Sy} \sin(\Omega_S t + \phi_S), \tag{23b}$$

where

$$\Theta_{Sx} = \Theta_{Sy} = 0.5 \tan^{-1}\left(\frac{r_S}{z_0}\right), \tag{23c}$$

then a slightly elliptical profile results which can clearly be observed by substituting equations (23a,b&c) into equations (21a&b) and is shown, normalised to the intended scan radius, in Figure 10a. Figure 10b shows the normalised actual scan radius as a function of scan angle.

Figure 10a clearly shows the inherent problem. When employing equal amplitude mirror drive signals, the probe laser beam does not follow the intended circular path.

For this particular combination of mirror separation and Laser Vibrometer stand-off, the maximum absolute error in the actual scan radius is of the order of 5%, as illustrated in Figure 10b. In addition to this, if the target surface is not flat and/or not perpendicular to the scanning system axis then, as for a straight-line scan, there will be a further (small) distortion in the scan profile. The effect of any probe laser beam position error is clearly structure dependent but, in some cases, there may be a significant difference between the velocities at the intended and actual measurement points.

3.3.2. Corrected Deflection Mirror Scan Angles

The elliptical shape in the scan trajectory resulting from the use of equal amplitude mirror drive signals can be overcome to an extent by accounting for the difference between the target to *x* mirror and target to *y* mirror distances and using "corrected" mirror drive signals with unequal amplitudes, i.e.:

$$\Theta_{Sx} = 0.5 \tan^{-1}\left(\frac{r_S}{z_0 + d_S}\right) \tag{24a}$$

and

$$\Theta_{Sy} = 0.5 \tan^{-1}\left(\frac{r_S}{z_0}\right). \tag{24b}$$

As illustrated in Figure 11, which shows the normalised scan radius as a function of scan angle for this corrected mirror drive signal case, the maximum absolute error in the actual scan radius is reduced to less than 0.05% by employing mirror drive signals with unequal amplitudes and this may be advantageous in some cases. Generally more important, however, is the influence that the variation in laser beam orientation during scanning has on the Laser Vibrometer measurement and this will be discussed in the following section.

3.4. VELOCITY MEASURED BY A DUAL MIRROR SCANNING LASER VIBROMETER

Using equation (17) as a direct alternative to equation (1) and evaluating the principal unit vector coefficients enables equation (5) to be re-expressed in terms of the deflection mirror scan angles:

$$\begin{aligned} U_m &= \sin 2\theta_{Sx}\left[\dot{x}_r(P_0)+\dot{x}_f(P)\right] \\ &\quad -\cos 2\theta_{Sx}\sin 2\theta_{Sy}\left[\dot{y}_r(P_0)+\dot{y}_f(P)\right] \\ &\quad +\cos 2\theta_{Sx}\cos 2\theta_{Sy}\left[\dot{z}_r(P_0)+\dot{z}_f(P)\right]. \end{aligned} \tag{25}$$

The known point x coordinate, x_0, can be slightly redefined for convenience such that it excludes the component Δx_0, given by equation (19), and equations (6b&c) are therefore re-formulated as follows:

$$\dot{y}_r(P_0) = \dot{y} + (\dot{\theta}_z + \Omega)(x_0 - d_S \tan 2\theta_{Sx} - x) - (\dot{\theta}_x + \Omega\theta_y)(z_0 - z) \tag{26a}$$

and

$$\dot{z}_r(P_0) = \dot{z} + (\dot{\theta}_x + \Omega\theta_y)(y_0 - y) - (\dot{\theta}_y - \Omega\theta_x)(x_0 - d_S \tan 2\theta_{Sx} - x). \tag{26b}$$

Derivation of equation (25) represents a significant development of the theoretical velocity sensitivity model as it allows the user to predict the sensitivity of a scanning Laser Vibrometer measurement for any combination of mirror scan angles on any target. It readily accommodates time dependent mirror scan angles where scanning profiles result and this will discussed in the following sections for some of the scanning arrangements that have been found to be useful in practice.

3.4.1. Circular Scans for Rotating Targets

Use of equation (25) allows prediction of the measured velocity in this particularly complex configuration with ease and it also shows how additional components can occur when performing “circular” scanning measurements on rotating targets.

The additional measurement components that occur in an "equal amplitude circular" scan can be quantified by substituting equations (23,b&c) into equation (25) and setting the flexible and rigid vibration components to zero. The system arrangement is as discussed earlier, i.e. the scanning system and target reference frames are collinear (no translational or angular misalignment), such that the measured Laser Vibrometer signal per unit rotation speed for this "no target vibration, no misalignment" case is given by:

$$\frac{U_m}{\Omega} = -d_S \sin\left(\tan^{-1}\left(\frac{r_S}{z_0} \right) \cos\left(\Omega_S t + \phi_S\right) \right) \sin\left(\tan^{-1}\left(\frac{r_S}{z_0} \right) \sin\left(\Omega_S t + \phi_S\right) \right). \qquad (27)$$

The additional information that exists in the measured Laser Vibrometer signal occurs at twice and six times the *scan* frequency, as shown in Figure 12. For typical rotation frequencies and scan radii, the level of the component at six times the scan frequency is well below the noise floor that results from the laser speckle effect, generally higher than 10^{-2}mm/s (10^{-4}mm/s/rad/s in Figure 12), and can therefore be considered insignificant. The component at twice the scan frequency is, however, of some significance since typical levels are of the order of mm/s. This component has been observed previously [16] but without full explanation until now.

Similarly, the additional measurement components that occur in a "corrected amplitude circular" scan can easily be quantified, in this case by substituting equations (23a&b) and (24a&b) into equation (25) to give a corresponding expression for the measured velocity:

$$\frac{U_m}{\Omega} = -d_S \sin\left(\tan^{-1}\left(\frac{r_S}{z_0 + d_S} \right) \cos\left(\Omega_S t + \phi_S\right) \right) \sin\left(\tan^{-1}\left(\frac{r_S}{z_0} \right) \sin\left(\Omega_S t + \phi_S\right) \right). \qquad (28)$$

Here, the additional information that exists in the measured Laser Vibrometer signal occurs at twice, four and six times the *scan* frequency, as shown in Figure 13. For typical rotation frequencies and scan radii, the level of the components at four and six

times the scan frequency can be considered insignificant. The component at 2x scan frequency is, however, still significant with typical levels only 5% lower, for this particular combination of d_S and z_0, than for the equal amplitude case.

It is due to additional measured "vibration" components such as this that care must be taken when interpreting vibration information obtained from such measurements. This issue demonstrates the value of the velocity sensitivity model very clearly – it enables the vibration engineer to make Laser Vibrometer measurements with confidence. Theoretical component amplitudes show good agreement with those obtained from experimentation and with those that have been previously reported [16] and a full experimental validation will be the subject of a subsequent publication. The model can also be used to examine the effects of misalignment between the target and scanning system axes and this will also be explored in the same subsequent publication.

"Circular tracking" measurements can be arranged for by using a corrected amplitude circular scan and setting the scan frequency equal to the target rotation frequency such that the probe laser beam remains fixed on a single point on the target during rotation. The model continues to predict the additional components encountered that, in this case, occur at twice, four and six times *rotation* frequency.

3.4.2. Small-Scale Circular Scans for Non-Rotating Targets

"Small-scale circular scans" on non-rotating targets have proved useful in previous work [6]. In this application, the illuminated region is assumed to move as a rigid body. In such a case, small angle approximations apply and the measured velocity, combining equations (25), (6a) and (26&c), is given by:

$$U_m = \left\{2\theta_{Sx}\dot{\theta}_y z_0 + 2\theta_{Sy}\dot{\theta}_x z_0 + \dot{z}\right\} + \left\{\begin{array}{l} 2\theta_{Sx}\left[\dot{x} + \theta_z y - \dot{\theta}_y z\right] \\ \quad -2\theta_{Sy}\left[\dot{y} - \dot{\theta}_z\left(d_S 2\theta_{Sx} + x\right) - \dot{\theta}_x z\right] + \left[-\dot{\theta}_x y + \dot{\theta}_y\left(d_S 2\theta_{Sx} + x\right)\right] \end{array}\right\}, \quad (29)$$

in which the typically larger terms are those in the first set of braces. For single frequency vibrations, the resulting frequency spectrum contains a component at the vibration frequency, ω, and sidebands at $\omega \pm \Omega_S$. The component at ω is due to $\dot{z}$ whilst the sideband components result from the products $\theta_{Sx}\dot{\theta}_y$ and $\theta_{Sy}\dot{\theta}_x$. The amplitudes and phases of the sidebands can be resolved to give $\dot{\theta}_x$ and $\dot{\theta}_y$.

As the diameter of the scan is increased, assuming small angle approximations still apply, further terms (from the second set of braces) become significant. For example, the resulting spectrum will contain a second pair of sidebands, at $\omega \pm 2\Omega_S$, due to the product $\theta_{Sy}\dot{\theta}_z\theta_{Sx}$.

3.4.3. Conical Scans for Non-Rotating Targets

The velocity sensitivity analysis set out in terms of deflection mirror scan angles has enabled a detailed examination of actual rather than idealised scan configurations. As a final example, the especially complex case of a conical scanning measurement will be investigated. As a means of emphasising the usefulness of the velocity sensitivity model, the differences between a truly conical scan, which can only be achieved using an idealised scanning system, and a dual mirror "conical" scan can be examined in detail.

With reference to Figure 14, a conical scan can be performed via the introduction of a positive lens between the target and the scanning Laser Vibrometer. A lens, of focal length *f*, is positioned with its optical axis coincident with the scanning system optical axis at a distance of z_0 from the *y* deflection mirror. Since the laser beam direction, before incidence on the lens, is not parallel with the optical axis, the user would typically place the target in the image plane that is a distance of z_1 from the lens. The difference between z_1 and *f*, which is likely to be negligible in practice, is exaggerated in

Figure 14 for clarity. In this dual mirror scanning system case, this results in the laser beam incidence point scanning back and forth in the *x* direction on the target surface (also exaggerated in Figure 14), in sympathy with the beam incidence point on the *y* mirror, and the scanned volume is not truly conical.

The direction of the laser beam after passing through the lens, defined in this case by the unit vector $\hat{b}_1$, can be evaluated by considering the beam path between the lens and the target and forming the following vector equation:

$$\left[x_S + \frac{z_1}{z_0}\Delta x_0\right]\hat{x} + [y_S]\hat{y} + [z_1]\hat{z} = \left[\sqrt{\left(x_S + \frac{z_1}{z_0}\Delta x_0\right)^2 + {y_S}^2 + {z_1}^2}\right]\hat{b}_1, \tag{30}$$

where x_S and y_S are as given in equations (21&b) and this incidence point of the laser beam on the lens is taken as the known point. This expression is relatively straightforward to rearrange for $\hat{b}_1$, forming an equivalent to equations (1) or (17). Evaluating the principal unit vector coefficients enables equation (5) to be re-expressed resulting in an expression specific to dual mirror, "conical" scanning LDV.

For the idealised scanning system, the laser beam incidence point remains fixed on the target, as shown in Figure 14. Here, the laser beam direction, defined by the unit vector $\hat{b}_1'$, can be evaluated from the following vector equation:

$$[x_S]\hat{x} + [y_S]\hat{y} + [z_1]\hat{z} = \left[\sqrt{{x_S}^2 + {y_S}^2 + {z_1}^2}\right]\hat{b}_1', \tag{31}$$

where x_S and y_S are as given in equation (22). Again, re-arranging for $\hat{b}_1'$ and evaluating the principal unit vector coefficients enables equation (5) to be re-expressed specific to idealised conical scanning LDV.

The differences between $\hat{b}_1$ and $\hat{b}_1'$ lead to measurable differences between the actual and intended Laser Vibrometer outputs and the velocity sensitivity model enables the

quantification of these differences. Figures 15a,b&c show measurement predictions for an idealised, dual mirror equal amplitude and dual mirror corrected amplitude conical scan, respectively, for a typical configuration where f = 50mm. The target is undergoing simultaneous unit vibrations in the x, y, and z directions at 10 times scan frequency (arbitrarily chosen).

For the idealised and equal amplitude dual mirror conical scans, the difference between the components at ω is 1.26% and the difference between the components at $\omega \pm \Omega_S$ is 1.36%. For the idealised and corrected amplitude dual mirror conical scans, the difference between the components at ω is 0.05% and the difference between the components at $\omega \pm \Omega_S$ is 0.06%. This reduction is significant and may be beneficial in some situations. Both dual mirror measurements also contain several additional sidebands compared to the idealised measurement which may lead to complications in analysis, for example when dealing with more complex target vibrations.

This example shows how, even for the most complex of scanning configurations, the velocity sensitivity model can readily predict the Laser Vibrometer output.

CONCLUSIONS

The original derivation of the comprehensive velocity sensitivity model showed explicitly how the velocity sensed by an arbitrarily orientated laser beam incident on a rotating target, of rigid cross-section, undergoing arbitrary vibration, is dependent upon both the target velocity components and the direction of the laser beam. This was extended in this paper to include provision for targets with flexible cross-sections, since Laser Vibrometer measurements are generally employed on such targets.

The use of Laser Vibrometers incorporating some form of manipulation of the laser beam orientation, typically using two orthogonally aligned mirrors, has become

increasingly popular in recent years. Considerable attention has been given to the operation of such scanning Laser Vibrometers in continuous scanning mode in which the laser beam orientation is a continuous function of time. This paper has investigated the application of the velocity sensitivity model to these particularly challenging measurement configurations. A major novel development was the reformulation of the original model in terms of mirror scan angles, rather than laser beam orientation angles, which is especially useful since it is these angles that an operator would seek to control in practice. This proved to be extremely beneficial in incorporating the complexity of real scanning configurations and allowed easy formulation of measured velocity, revealing some important details in the measurement that were not apparent in predictions based on an idealised model of the scanning arrangement.

The revised velocity sensitivity model has been applied in this paper to show how the common use of a pair of orthogonally aligned scanning mirrors leads to a significant yet predictable additional component in the Laser Vibrometer output at twice the scan frequency in circular scanning measurements on rotating targets. Furthermore, it has been shown how the combination of this mirror configuration and equal amplitude cosine and sine mirror drive functions leads to an elliptical scan profile. Corrected amplitude drive signals can be employed to overcome this elliptical profile to an extent but the amplitude of the additional component at twice the scan frequency is not significantly reduced.

For the especially complex cases of small-scale circular and conical scans on non-rotating targets, implementation of the model enabled a detailed examination of the differences between idealised and actual scanning configurations. In particular, the origins of all of the components that occur in the measured data due to instrument

configuration were easily revealed and an analysis of their influence on the measurement was presented.

This paper has shown how, even for the most complex of Laser Vibrometer measurement configurations, the velocity sensitivity model can straightforwardly predict the instrument output, thereby enabling the vibration engineer to make LDV measurements with confidence.

ACKNOWLEDGEMENT

The authors would like to acknowledge the support of the Engineering and Physical Sciences Research Council who are funding this project.

REFERENCES

1. N. A. HALLIWELL in D. C. WILLIAMS (ed.) 1993 *Optical Methods in Engineering Metrology* (London: Chapman & Hall), 179-211. Chapter 6 – Laser Vibrometry.

2. P. SRIRAM, J. I. CRAIG and S. HANAGUD 1990 *The International Journal of Analytical and Experimental Modal Analysis* 5(3), 155-167. A scanning laser Doppler vibrometer for modal testing.

3. B. STOFFREGEN and A. FELSKE 1985 *Transactions of SAE – Technical Paper Series* 850327, 934-940. Scanning laser Doppler vibration analysis system.

4. B. JUNGE 1994 *Proceedings of SPIE – First International Conference on Vibration Measurements by Laser Techniques, Ancona, Italy* 2358, 377-382. Experiences with scanning laser vibrometry in automotive industries.

5. J. HANCOX, B. C. STAPLES and R. J. PARKER 1995 *Proceedings of IMechE – Journal of Aerospace Engineering* 209, 35-42. The application of scanning laser Doppler vibrometry in aero-engine development.

6. A. B. STANBRIDGE and D. J. EWINS 1999 *Mechanical Systems and Signal Processing* 13(2), 255-270. Modal testing using a scanning laser Doppler vibrometer.

7. R. BARRON 1996 *Engineering Condition Monitoring* (Harlow: Addison Wesley Longman.

8. A. F. P. SANDERSON 1992 *Proceedings of IMechE – Fifth International Conference on Vibrations in Rotating Machinery, Bath, U.K.* 1992-6, pp263-273. The vibration behaviour of a large steam turbine generator during crack propagation through the generator rotor.

9. Q. V. DAVIS and W. K. KULCZYK 1969 *Nature* 222, 475-476. Vibrations of turbine blades by means of a laser.

10. T. A. RIENER, A. C. GODING and F. E. TALKE 1988 *IEEE Transactions on Magnetics* 24(6), 2745-2747. Measurement of head/disc spacing modulation using a two channel fiber optic laser Doppler vibrometer.

11. R. W. WLEZEIN, D. K. MIU and V. KIBENS 1984 *Optical Engineering* 24(4), 436-442. Characterization of rotating flexible disks using a laser Doppler vibrometer.

12. R. A. COOKSON and P. BANDYOPADHYAY 1980 *Transactions of ASME – Journal of Engineering for Power* 102, 607-612. A fiber-optics laser Doppler probe for vibration analysis of rotating machines.

13. A. K. REINHARDT, J. R. KADAMBI and R. D. QUINN 1995 *Transactions of ASME – Journal of Engineering for Gas Turbines and Power* 117, 484-488. Laser vibrometry measurements on rotating blade vibrations.

14. I. BUCHER, P. SCHMIECHEN, D. A. ROBB and D. J. EWINS 1994 *Proceedings of SPIE – First International Conference on Vibration Measurements by Laser Techniques, Ancona, Italy* 2358, 398-408. A laser-based measurement system for measuring the vibration on rotating discs.

15. A. B. STANBRIDGE and D. J. EWINS 1995 *Transactions of ASME – Design Engineering Technical Conference* 3(B), 1207-1213. Modal testing of rotating discs using a scanning LDV.

16. P. CASTELLINI and N. PAONE 2000 *Review of Scientific Instruments* 71(12), 4639-4647. Development of the tracking laser vibrometer: performance and uncertainty analysis.

17. S. J. ROTHBERG, J. R. BAKER and N. A. HALLIWELL 1989 *Journal of Sound and Vibration* 135(3), 516-522. Laser vibrometry: pseudo-vibrations.

18. S. J. ROTHBERG and N. A. HALLIWELL 1994 *Transactions of ASME – Journal of Vibration and Acoustics* 116(3), 326-331. Vibration measurements on rotating machinery using laser Doppler velocimetry.

19. T. J. MILES, M. LUCAS, N. A. HALLIWELL and S. J. ROTHBERG 1999 *Journal of Sound and Vibration* 226(3), 441-467. Torsional and bending vibration measurement on rotors using laser technology.

20. J. R. BELL and S. J. ROTHBERG 2000 *Journal of Sound and Vibration* 237(2), 245-261. Laser vibrometers and contacting transducers, target rotation and six degree-of-freedom vibration: what do we really measure?

LIST OF FIGURES

Figure 13 – Additional measurement components that occur in a dual-mirror circular scan when employing corrected amplitude cosine and sine mirror drive signals (r_S = 100mm, d_S = 50mm and z_0 = 1m)

Figure 14 – The conical scanning arrangement incorporating a positive lens

Figure 15 – Idealised (a), dual mirror equal amplitude (b) and dual mirror corrected amplitude (c) conical scanning Laser Vibrometer measurements on a target undergoing simultaneous vibration in the *x*, *y* and *z* directions

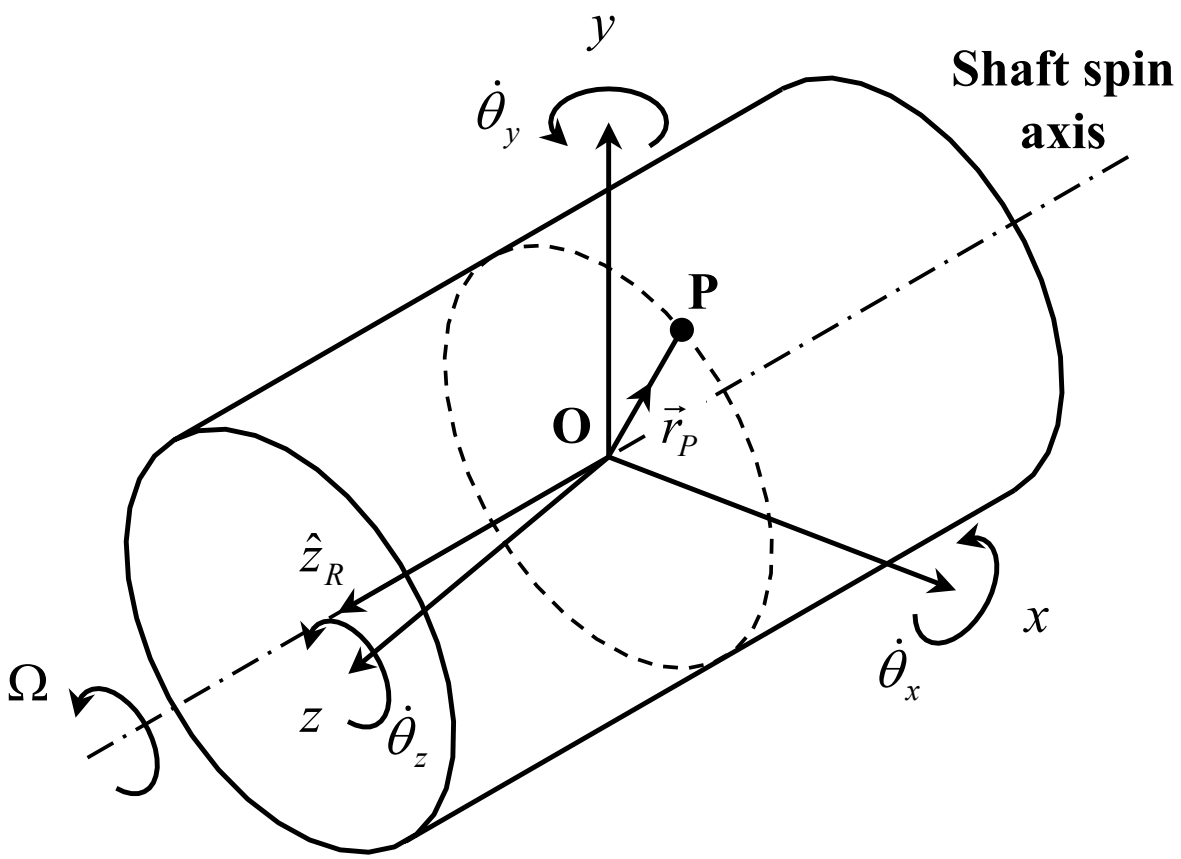

Figure 1
Vibration Measurements using
Continuous Scanning Laser Doppler Vibrometry:
Theoretical Velocity Sensitivity Analysis with Applications

Ben Halkon and Steve Rothberg
Wolfson School of Mechanical and Manufacturing Engineering
Loughborough University, Loughborough, LEICS., LE11 3TU

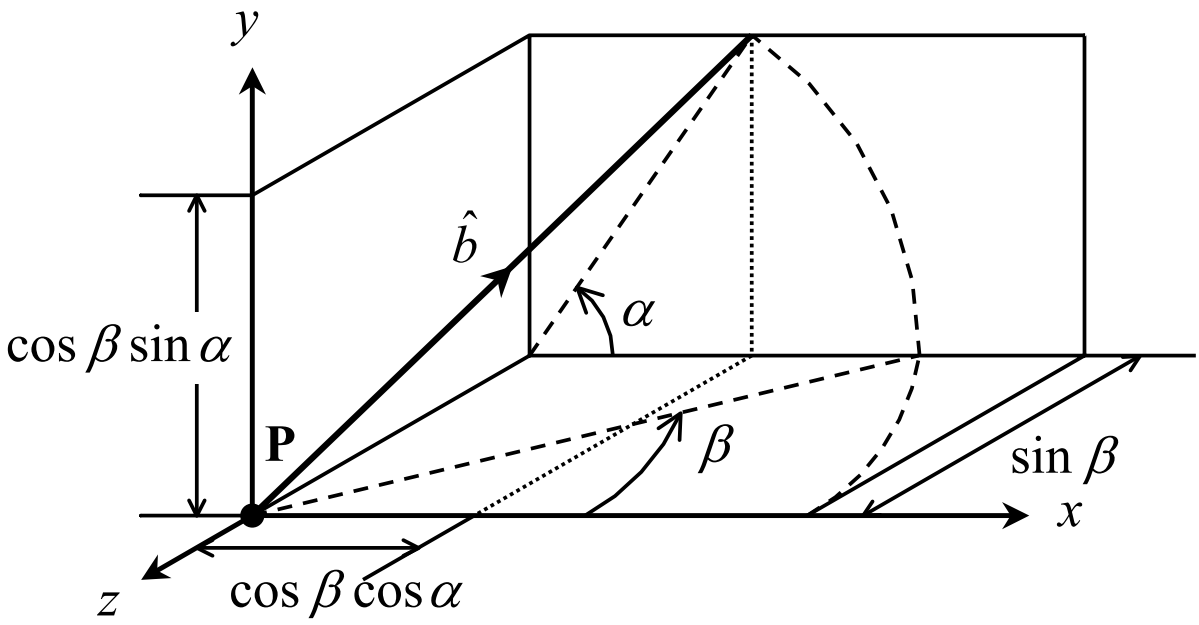

Figure 2
Vibration Measurements using
Continuous Scanning Laser Doppler Vibrometry:
Theoretical Velocity Sensitivity Analysis with Applications
Ben Halkon and Steve Rothberg
Wolfson School of Mechanical and Manufacturing Engineering
Loughborough University, Loughborough, LEICS., LE11 3TU

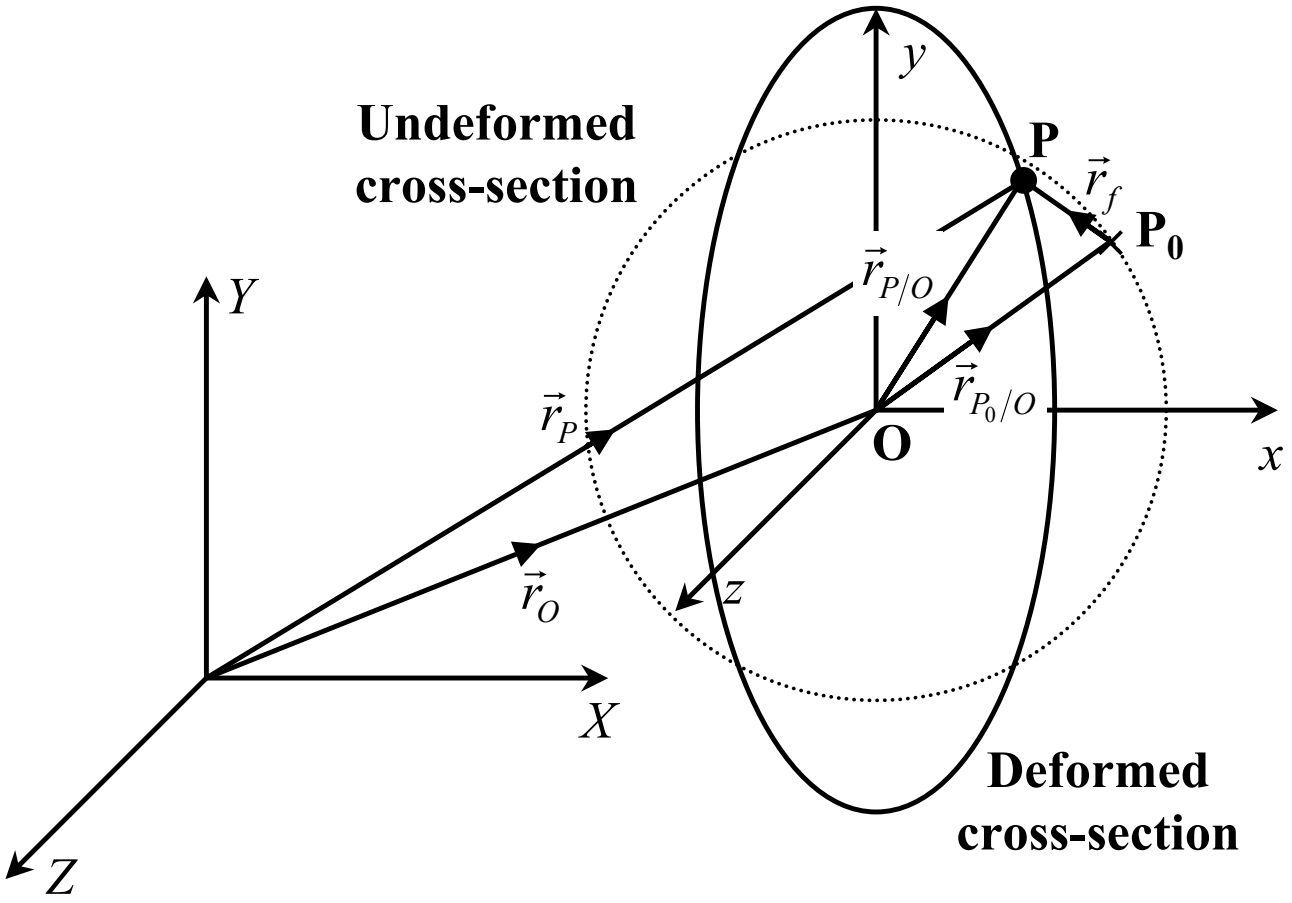

Figure 3
Vibration Measurements using
Continuous Scanning Laser Doppler Vibrometry:
Theoretical Velocity Sensitivity Analysis with Applications
Ben Halkon and Steve Rothberg
Wolfson School of Mechanical and Manufacturing Engineering
Loughborough University, Loughborough, LEICS., LE11 3TU

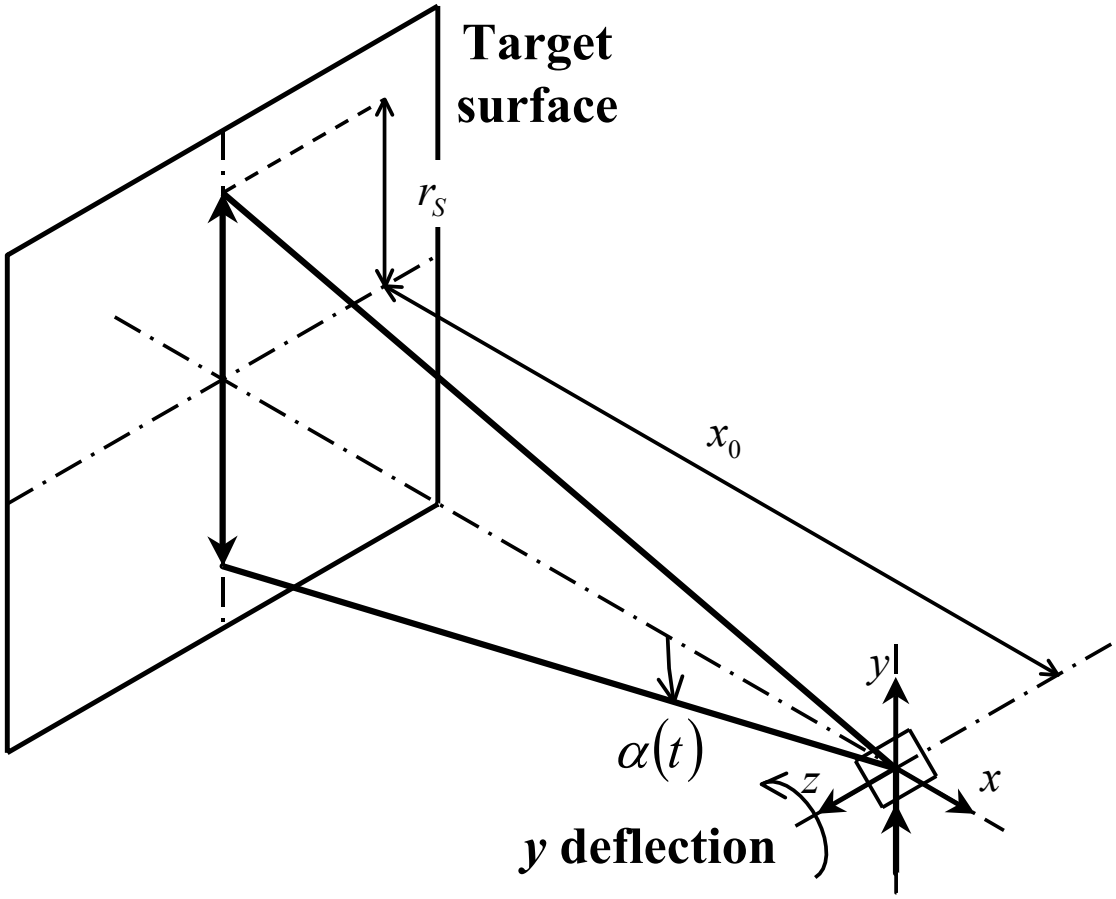

Figure 4
Vibration Measurements using
Continuous Scanning Laser Doppler Vibrometry:
Theoretical Velocity Sensitivity Analysis with Applications
Ben Halkon and Steve Rothberg
Wolfson School of Mechanical and Manufacturing Engineering
Loughborough University, Loughborough, LEICS., LE11 3TU

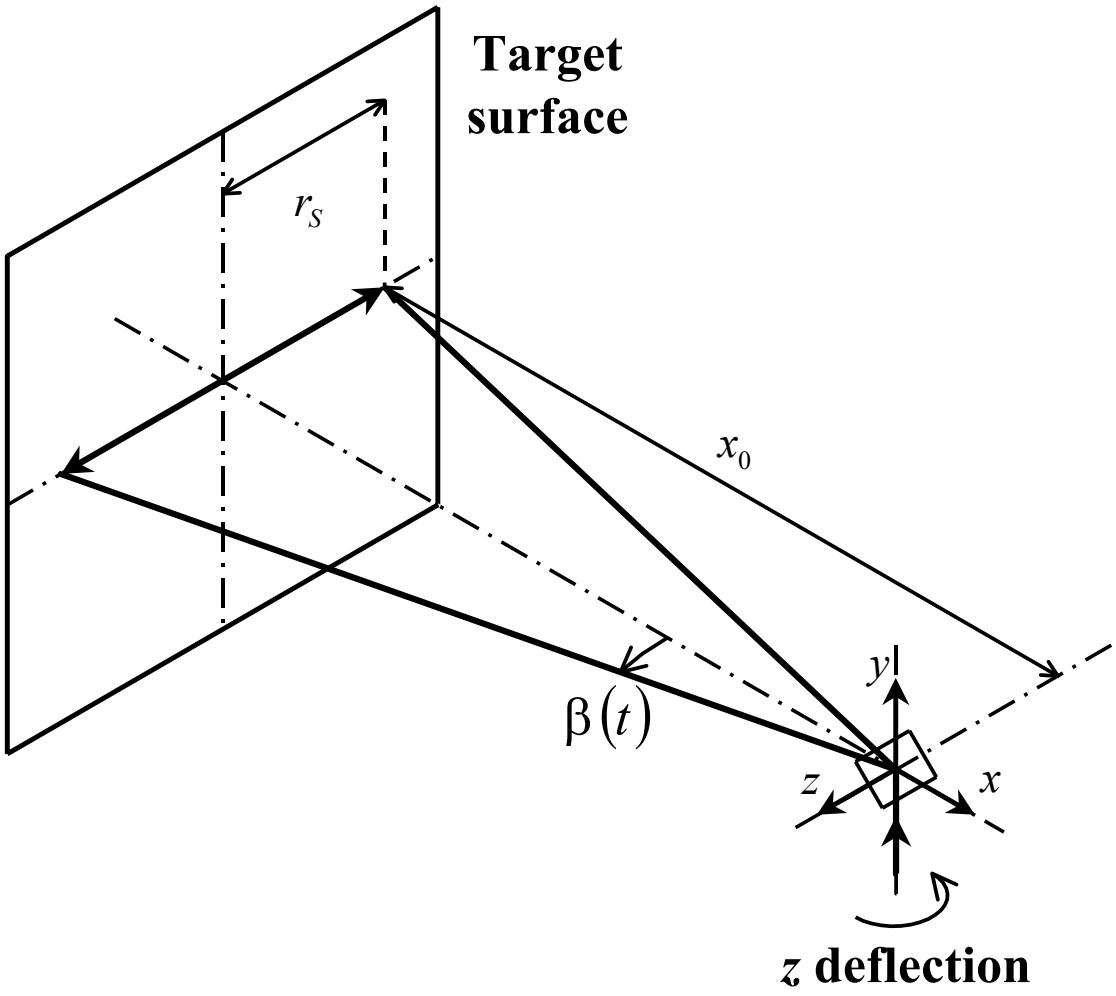

Figure 5
Vibration Measurements using
Continuous Scanning Laser Doppler Vibrometry:
Theoretical Velocity Sensitivity Analysis with Applications
Ben Halkon and Steve Rothberg
Wolfson School of Mechanical and Manufacturing Engineering
Loughborough University, Loughborough, LEICS., LE11 3TU

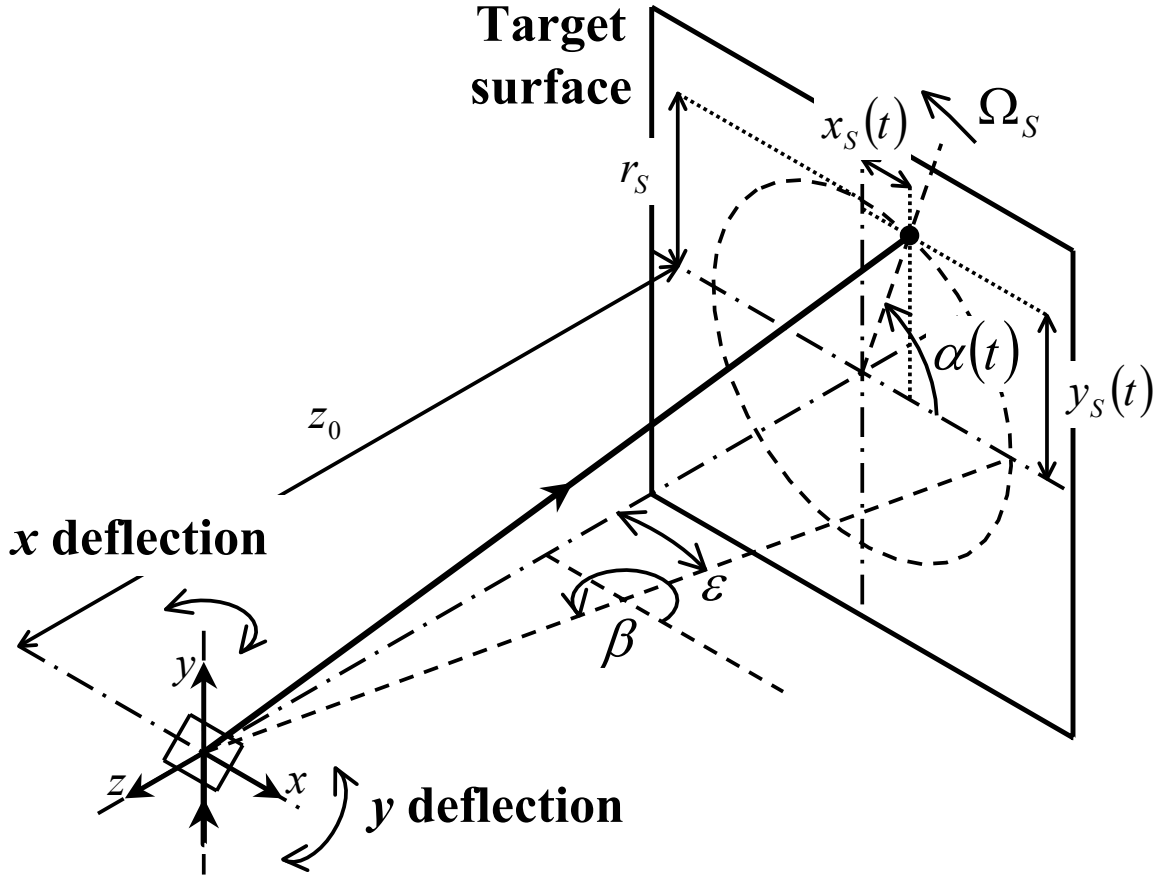

Figure 6
Vibration Measurements using
Continuous Scanning Laser Doppler Vibrometry:
Theoretical Velocity Sensitivity Analysis with Applications
Ben Halkon and Steve Rothberg
Wolfson School of Mechanical and Manufacturing Engineering
Loughborough University, Loughborough, LEICS., LE11 3TU

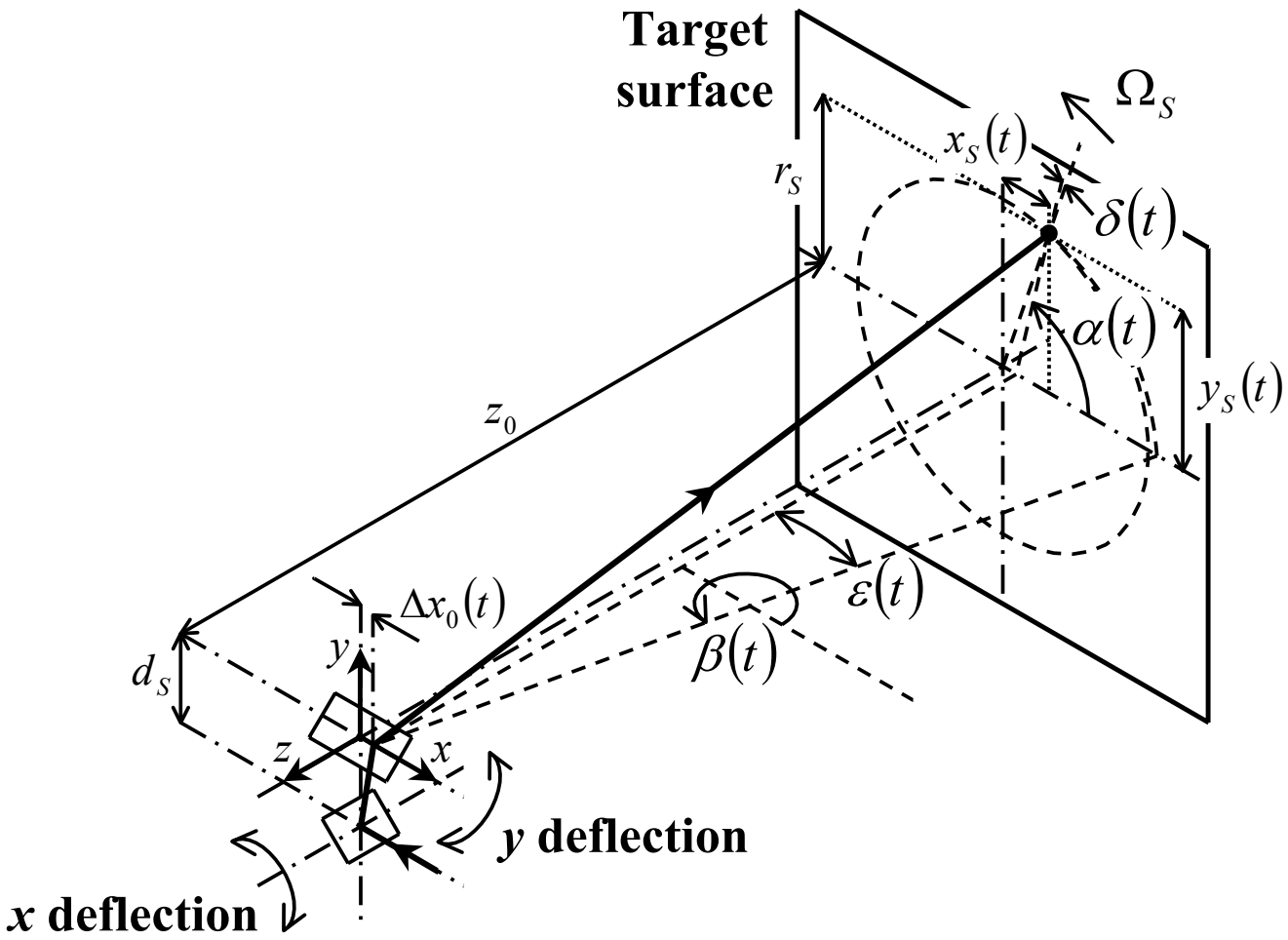

Figure 7
Vibration Measurements using
Continuous Scanning Laser Doppler Vibrometry:
Theoretical Velocity Sensitivity Analysis with Applications

Ben Halkon and Steve Rothberg
Wolfson School of Mechanical and Manufacturing Engineering
Loughborough University, Loughborough, LEICS., LE11 3TU

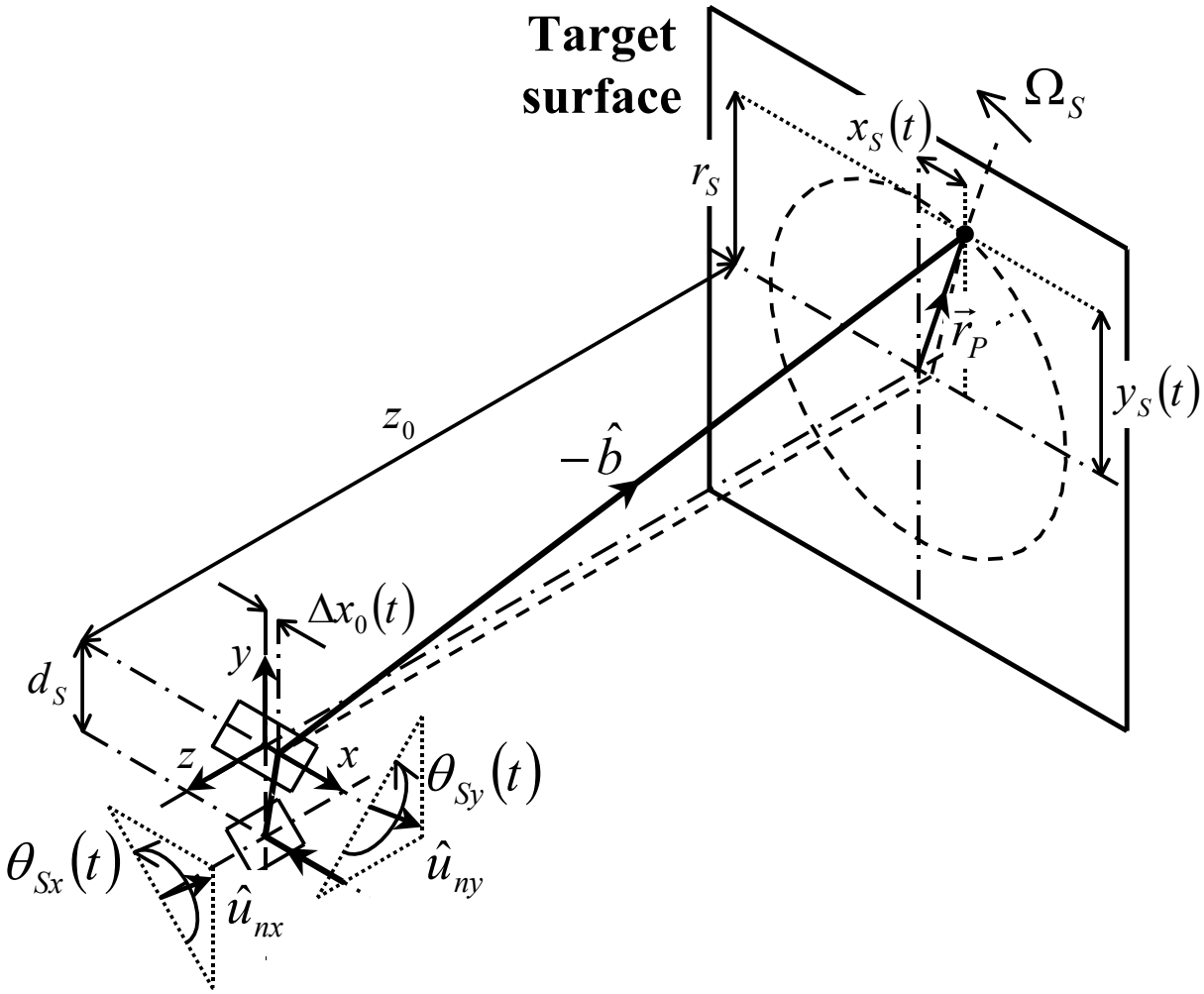

Figure 8
Vibration Measurements using
Continuous Scanning Laser Doppler Vibrometry:
Theoretical Velocity Sensitivity Analysis with Applications
Ben Halkon and Steve Rothberg
Wolfson School of Mechanical and Manufacturing Engineering
Loughborough University, Loughborough, LEICS., LE11 3TU

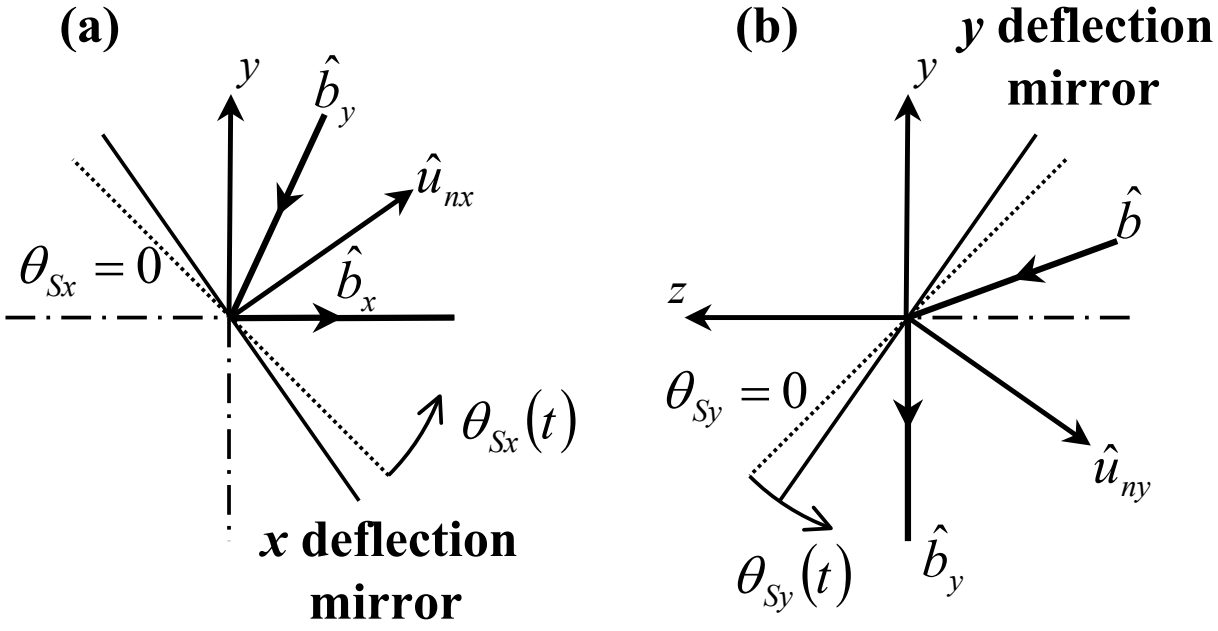

Figure 9
Vibration Measurements using
Continuous Scanning Laser Doppler Vibrometry:
Theoretical Velocity Sensitivity Analysis with Applications
Ben Halkon and Steve Rothberg
Wolfson School of Mechanical and Manufacturing Engineering
Loughborough University, Loughborough, LEICS., LE11 3TU

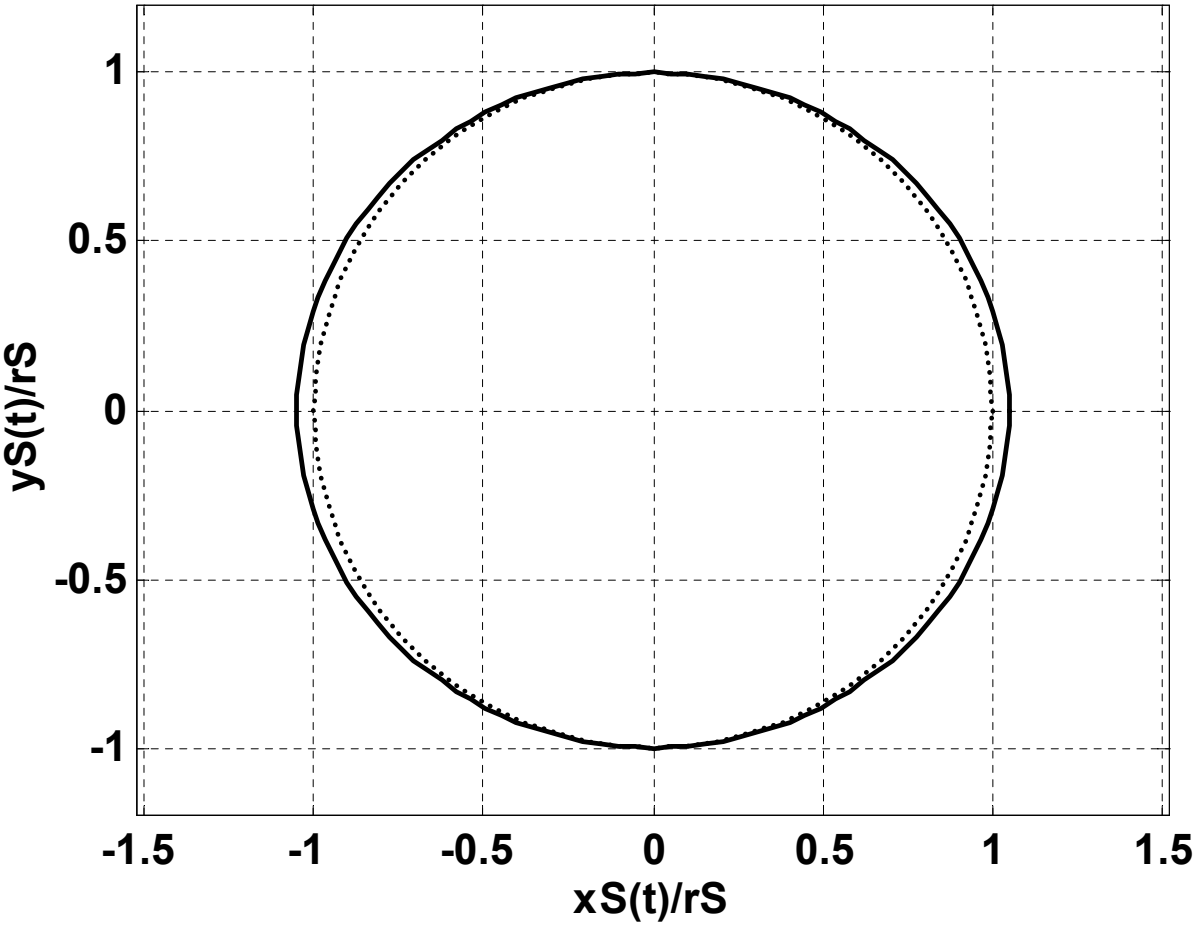

Figure 10a
Vibration Measurements using
Continuous Scanning Laser Doppler Vibrometry:
Theoretical Velocity Sensitivity Analysis with Applications
Ben Halkon and Steve Rothberg
Wolfson School of Mechanical and Manufacturing Engineering
Loughborough University, Loughborough, LEICS., LE11 3TU

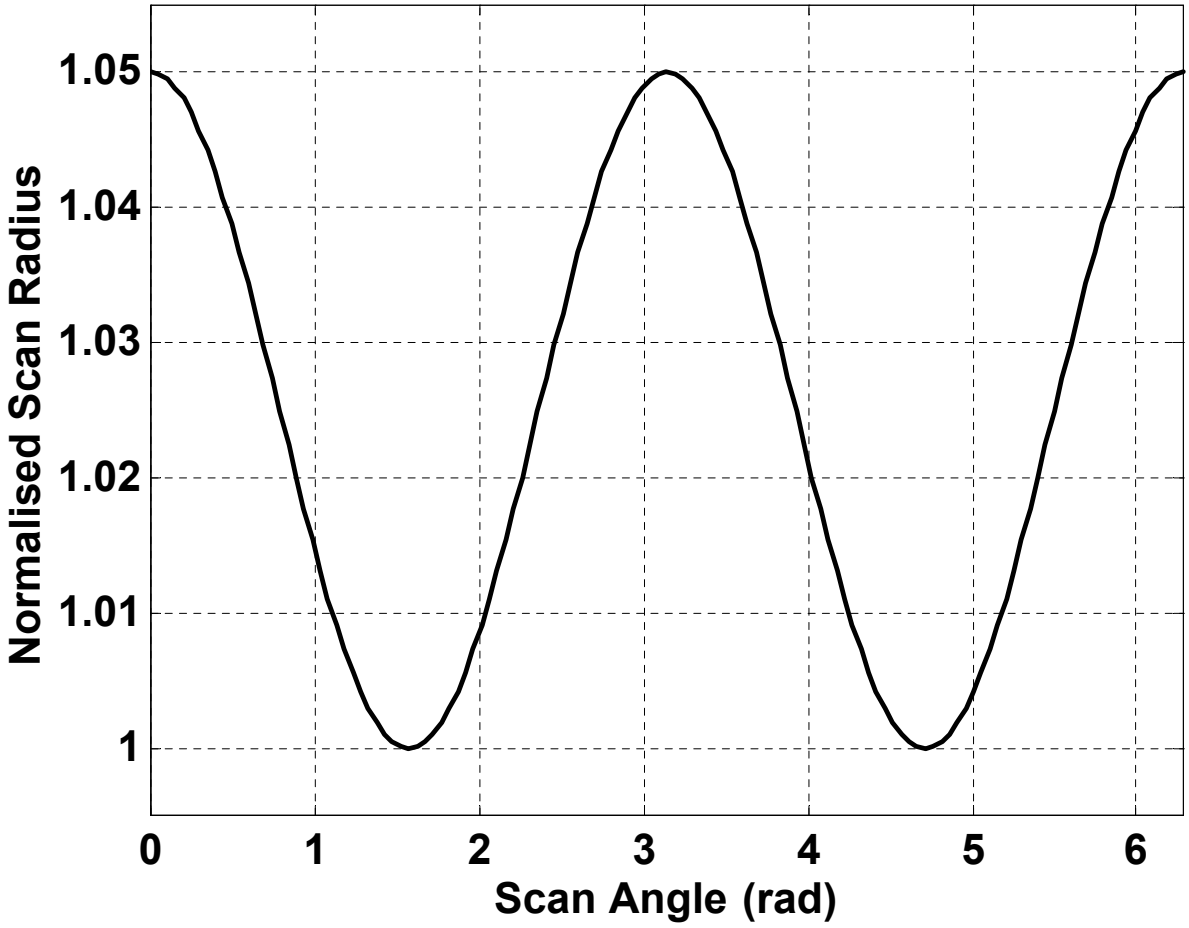

Figure 10b
Vibration Measurements using
Continuous Scanning Laser Doppler Vibrometry:
Theoretical Velocity Sensitivity Analysis with Applications
Ben Halkon and Steve Rothberg
Wolfson School of Mechanical and Manufacturing Engineering
Loughborough University, Loughborough, LEICS., LE11 3TU

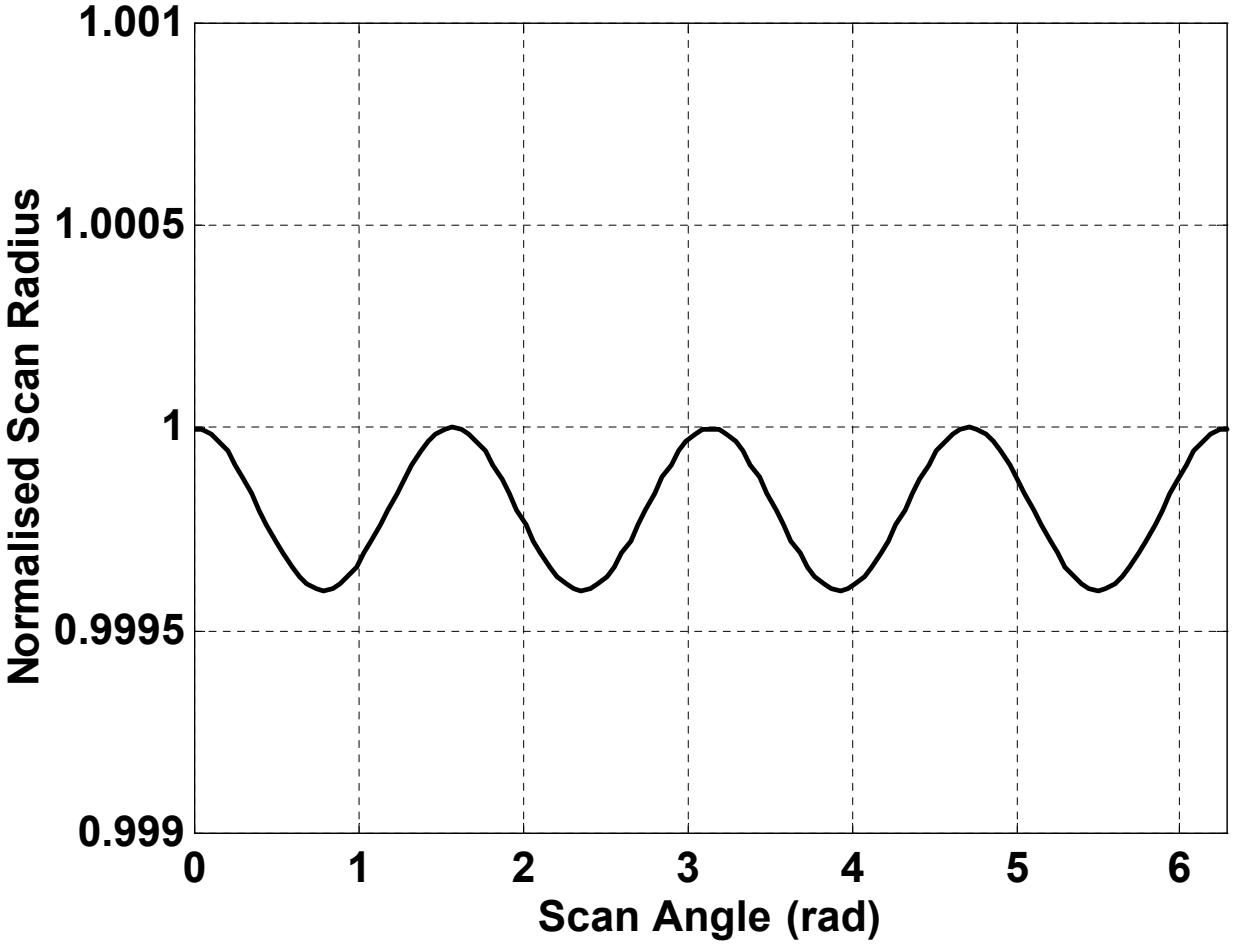

Figure 11
Vibration Measurements using
Continuous Scanning Laser Doppler Vibrometry:
Velocity Sensitivity Model Validation
Ben Halkon and Steve Rothberg
Wolfson School of Mechanical and Manufacturing Engineering
Loughborough University, Loughborough, LEICS., LE11 3TU

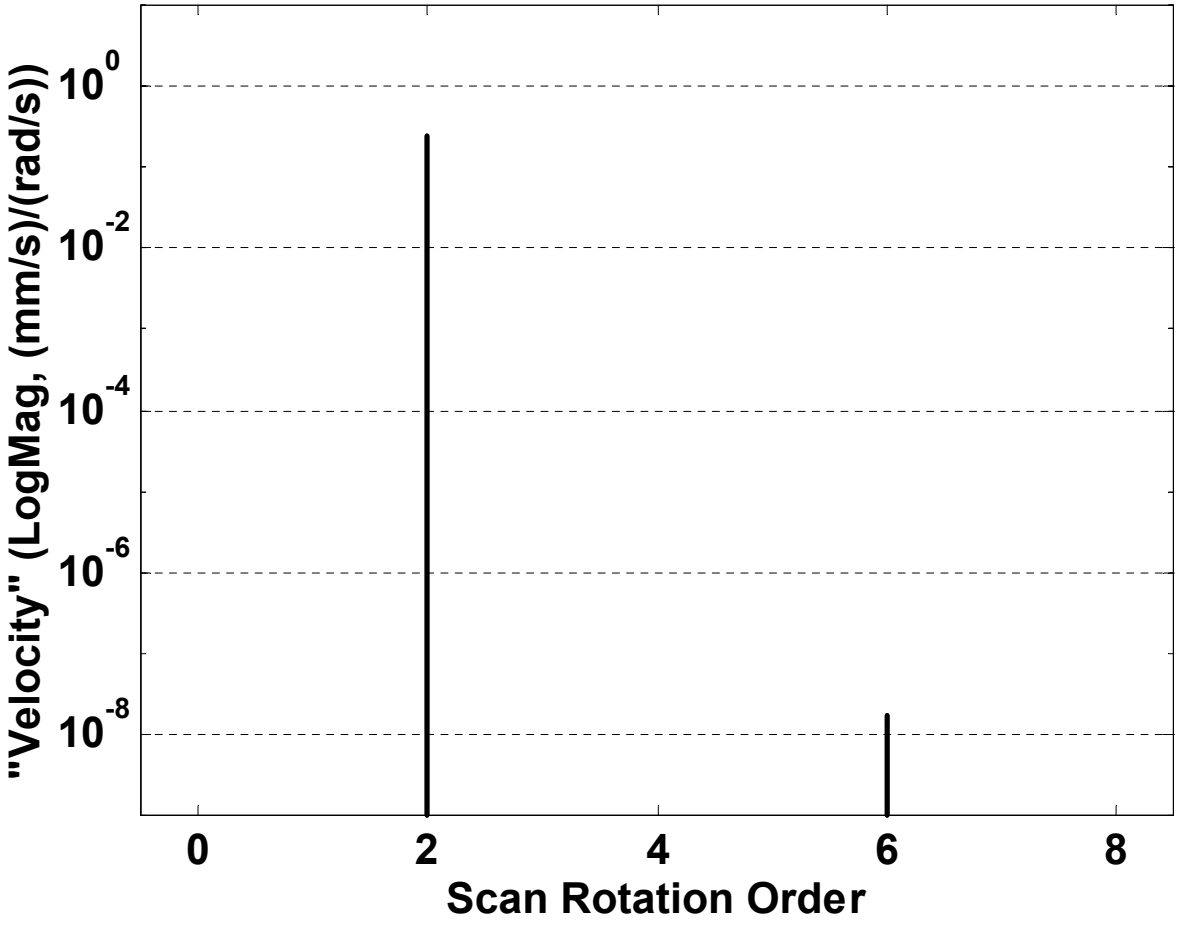

Figure 12
Vibration Measurements using
Continuous Scanning Laser Doppler Vibrometry:
Theoretical Velocity Sensitivity Analysis with Applications
Ben Halkon and Steve Rothberg
Wolfson School of Mechanical and Manufacturing Engineering
Loughborough University, Loughborough, LEICS., LE11 3TU

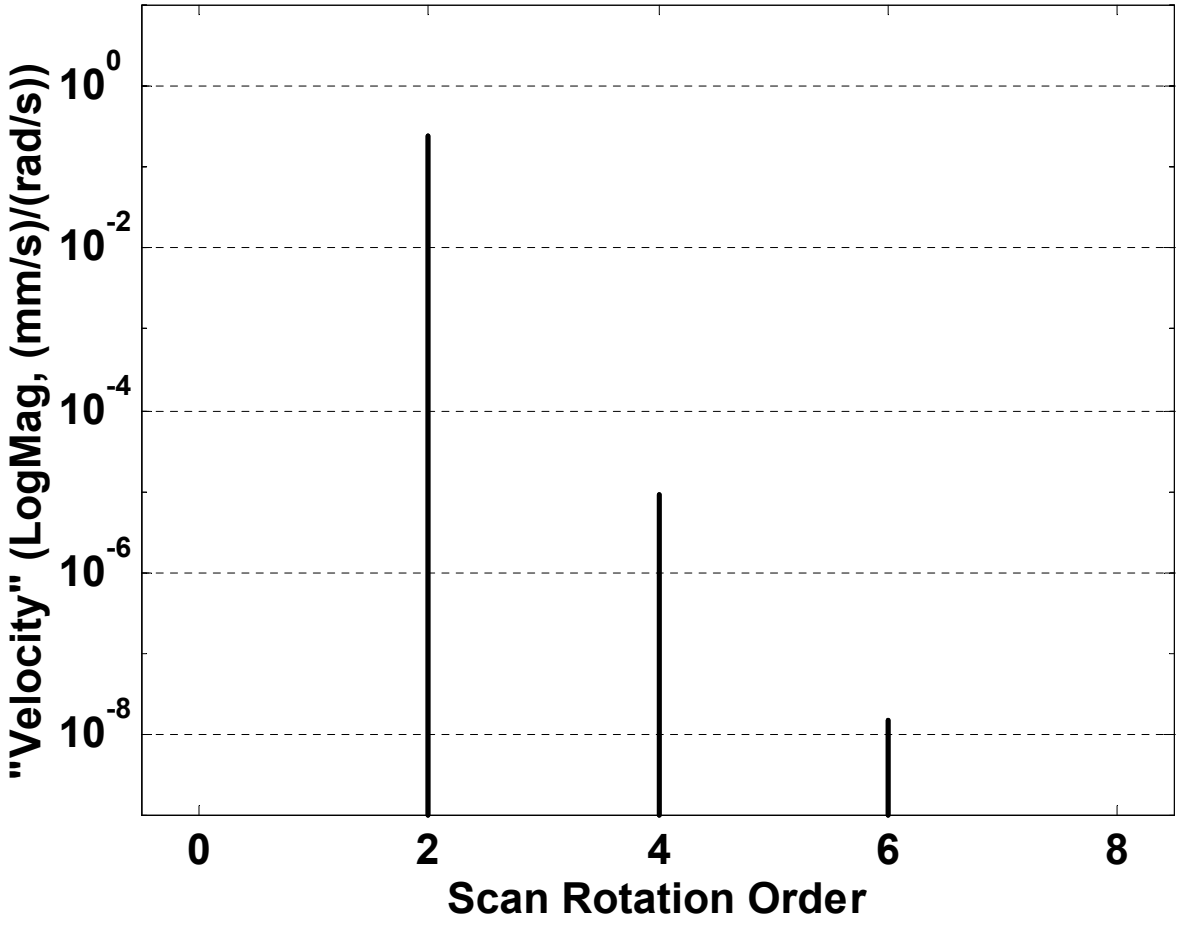

Figure 13
Vibration Measurements using
Continuous Scanning Laser Doppler Vibrometry:
Velocity Sensitivity Model Validation
Ben Halkon and Steve Rothberg
Wolfson School of Mechanical and Manufacturing Engineering
Loughborough University, Loughborough, LEICS., LE11 3TU

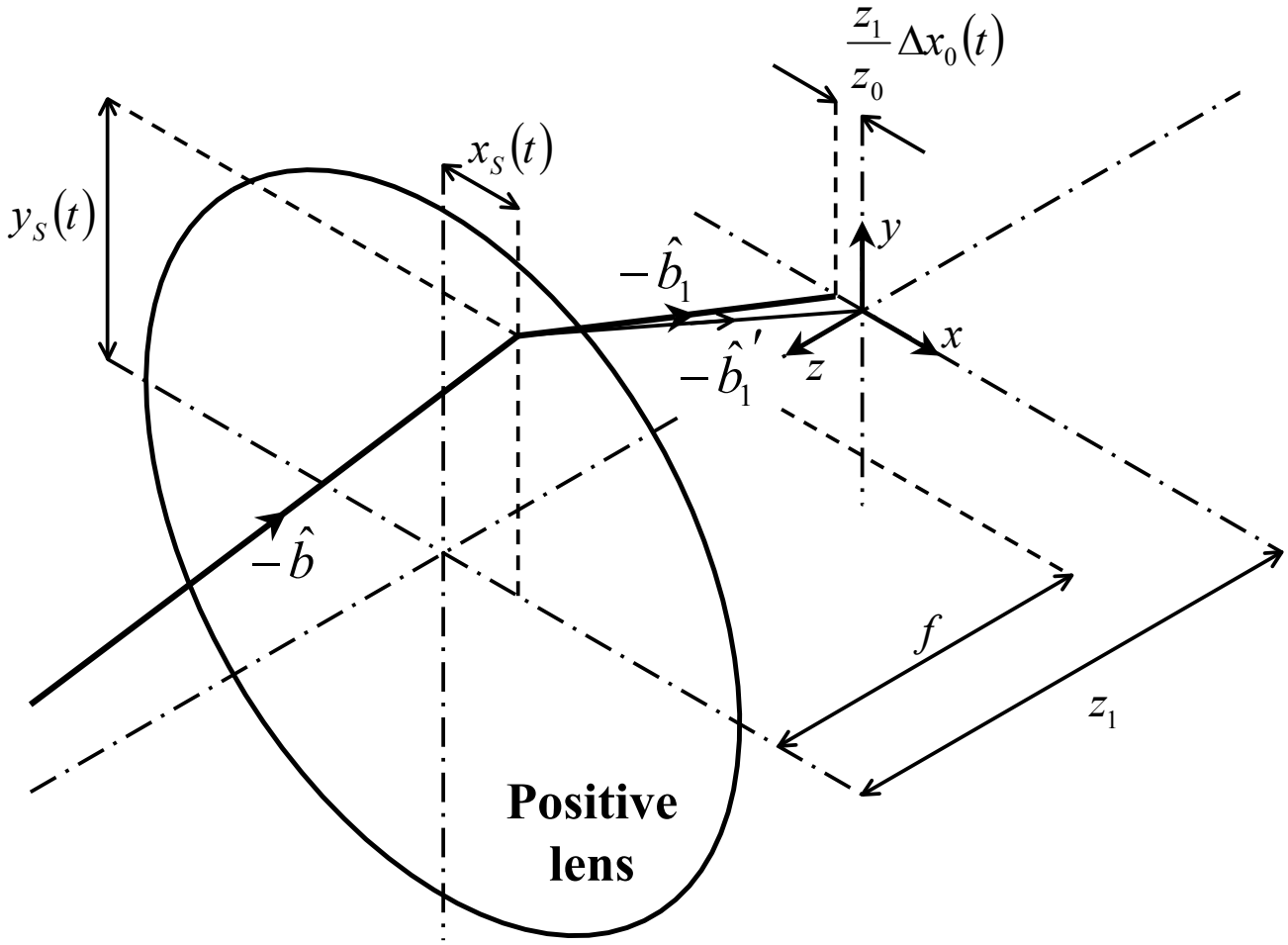

Figure 14
Vibration Measurements using
Continuous Scanning Laser Doppler Vibrometry:
Theoretical Velocity Sensitivity Analysis with Applications
Ben Halkon and Steve Rothberg
Wolfson School of Mechanical and Manufacturing Engineering
Loughborough University, Loughborough, LEICS., LE11 3TU

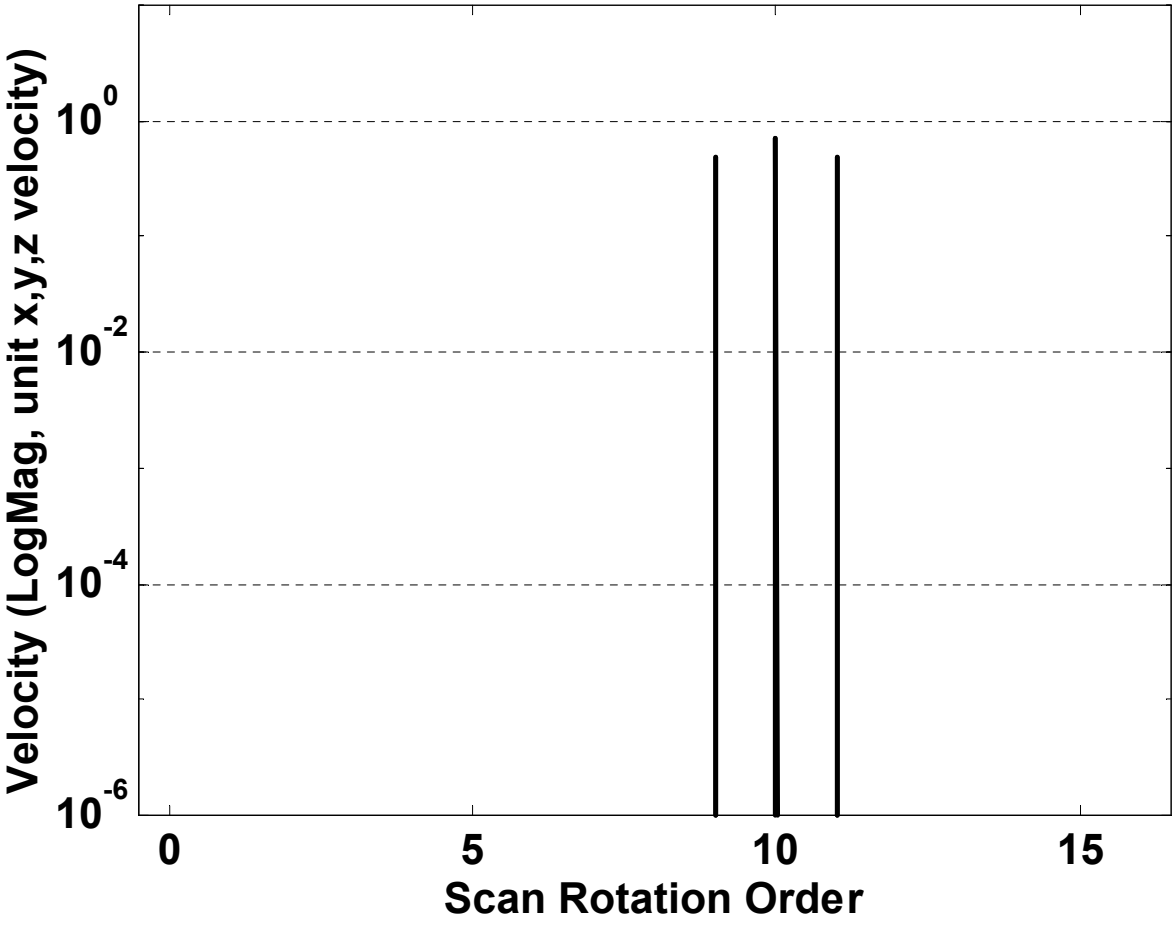

Figure 15a
Vibration Measurements using
Continuous Scanning Laser Doppler Vibrometry:
Theoretical Velocity Sensitivity Analysis with Applications
Ben Halkon and Steve Rothberg
Wolfson School of Mechanical and Manufacturing Engineering
Loughborough University, Loughborough, LEICS., LE11 3TU

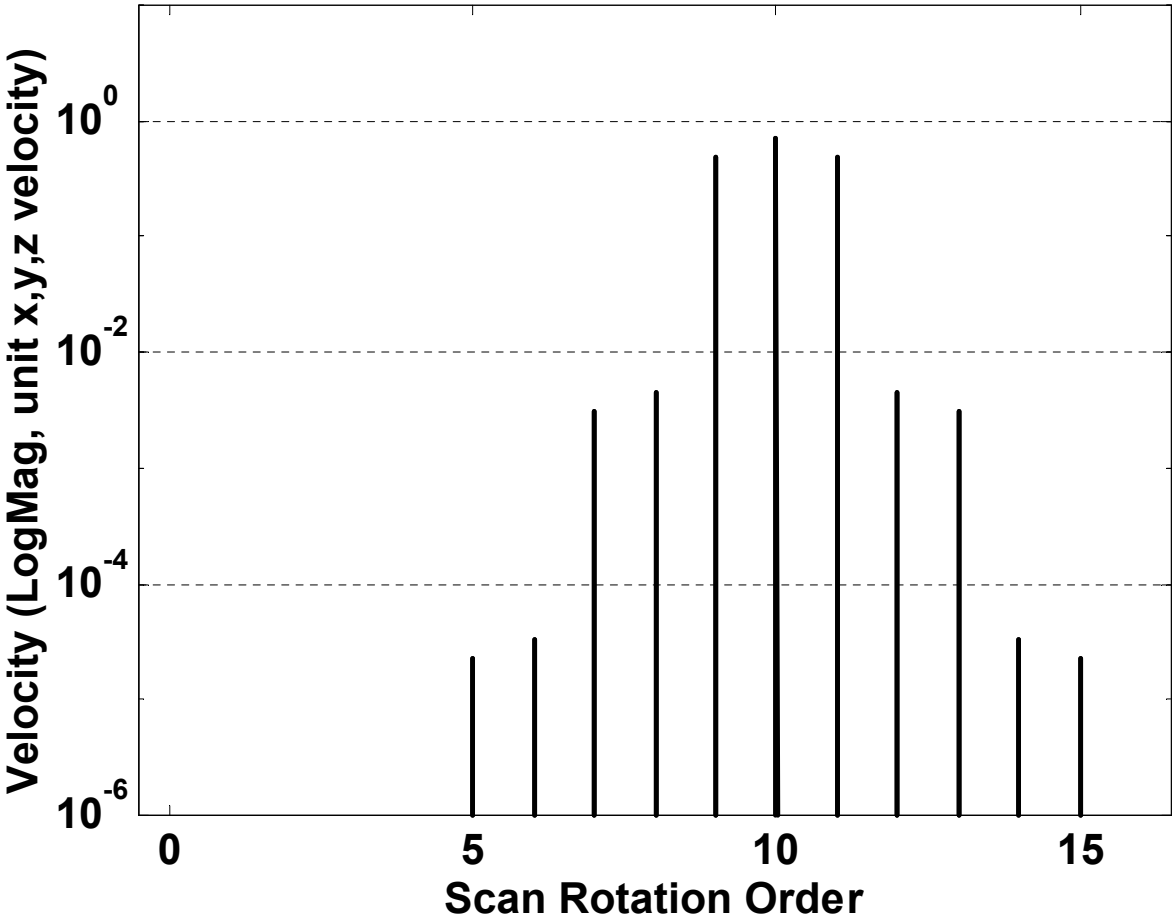

Figure 15b
Vibration Measurements using
Continuous Scanning Laser Doppler Vibrometry:
Theoretical Velocity Sensitivity Analysis with Applications
Ben Halkon and Steve Rothberg
Wolfson School of Mechanical and Manufacturing Engineering
Loughborough University, Loughborough, LEICS., LE11 3TU

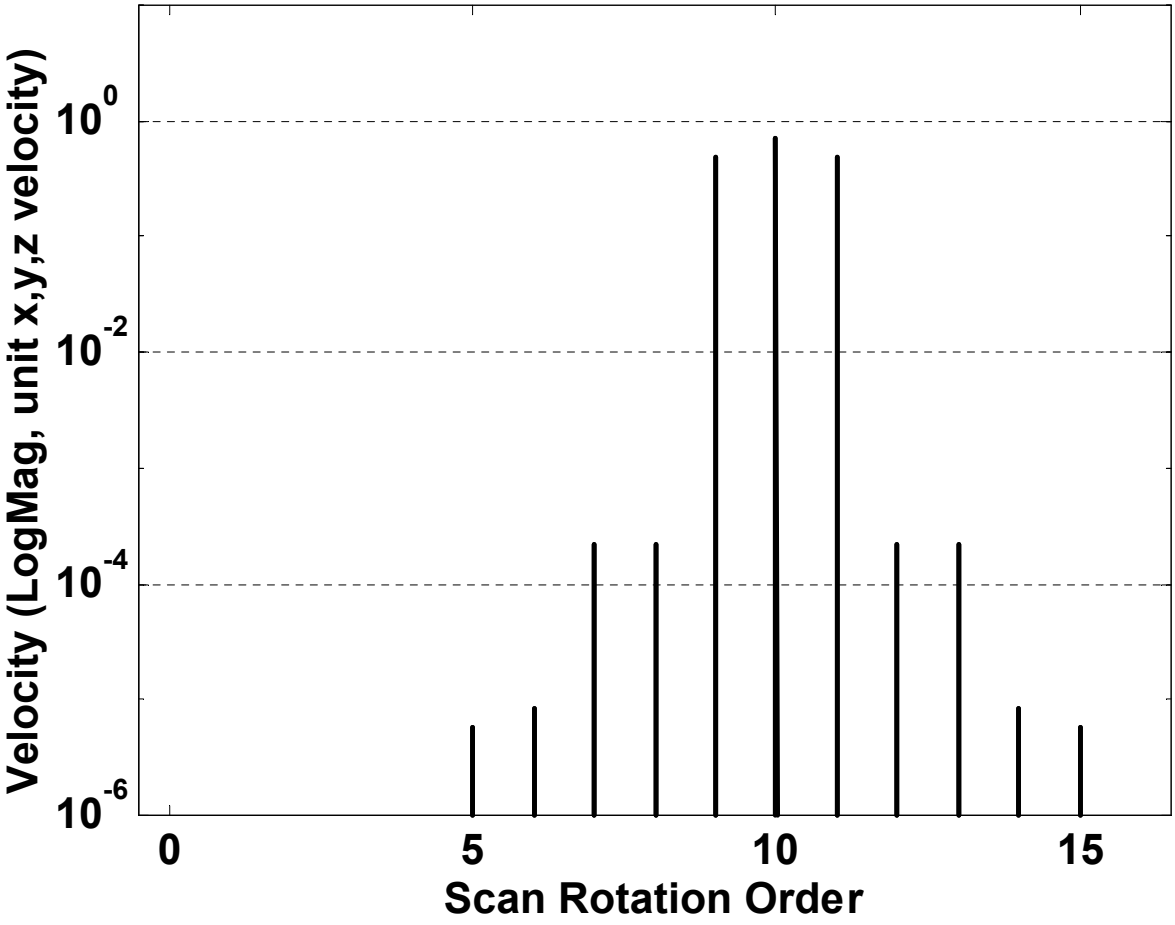

Figure 15c
Vibration Measurements using
Continuous Scanning Laser Doppler Vibrometry:
Theoretical Velocity Sensitivity Analysis with Applications
Ben Halkon and Steve Rothberg
Wolfson School of Mechanical and Manufacturing Engineering
Loughborough University, Loughborough, LEICS., LE11 3TU